A simplistic view of CONVECTION and WAVES in the **IFS** and in the **Indian Ocean**

with gratitude to IITM, Parthasarathi Mukhopadhyay and friends in India

A simplistic view of CONVECTION and WAVES in the **IFS** and in the **Indian Ocean**

Clear Air Turbulence

with **Martina Bramberger, Andreas Doernbrack (DLR)**

Nighttime convection and **Advection** of mesoscale systems
with **Tobias Becker**

Coupling with **Dynamics**

with **Sylvie Malardel**

Wave analysis: **Nedjeljka Zagar**, J. Dias, G. Kiladis
IFS convection in FV3**: Lisa Bengtsson**
Forecast busts: Dave Parssons
Kerala floods: **Parthasarathi Mukhopadhyay**

Convective Boundary-layer revision

with **Maike Ahlgrimm, Richard Forbes, Irina Sandu, Philippe Lopez**

Revised CIN/CAPE diagnostics
with **Ivan Tsonevski**

Analysing waves and turbulence (kinetic energy)

1. Hovmöller, simple **1D spectra and/or wavenumber-frequency spectra and co-spectra**, uni-variate. Then use filtering using shallow-water dispersion relations and regression to work out anomalies for other variables

2. **Fourier and wavelet analysis** , e.*g Chen-Ming et al (2010) Annal Geoph* for gravity waves produced by tropical cyclone

3. **Helmholtz decomposition of structure functions and spectra** calculated form aircraft data, *E. Lindborg (2015) J. Fl. Mech, Nastroem et al. (1984) JAS*

4. **Fitting 3D (gravity) wave vector** (amplitude, wavelength, direction) observations and model, e.g *P. Preusse et al. (2014) Atmos. Chem. Phys.*

5. **(Spectral) Empirical Orthogonal Function analysis**, eg. *O. Schmidt et al. (2019) Mon. Wea. Rev*

6. **Normal Mode analysis**, e.g. *Kasahari and Puri (1981), Žagar et al. (2009a,b,2012) MWR, (2015) Geosc. Mod. Develop*. In contrast to 1. this is a 3D multi-variate projection and requires the solution of M shallow water systems and the numerical solution of the vertical structure functions. Frequencies are obtained form dispersion relations for IG and Rossby waves

Challenge No1: Predicting Tropical large-scale waves: Example Aug 9-16 2018 (Kerala floods) and Sept 18-23 2019 anomalies

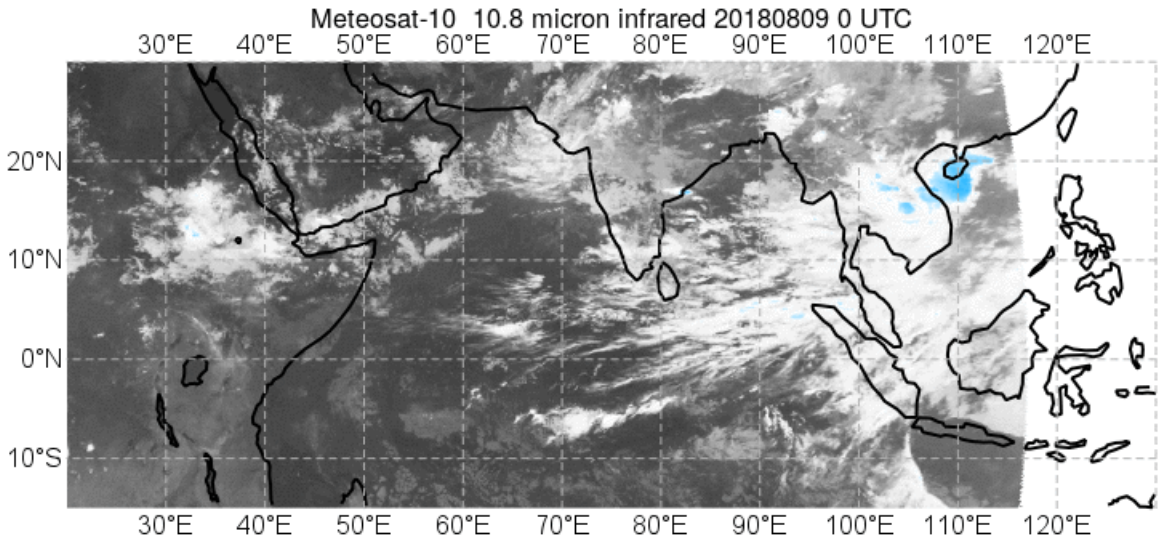

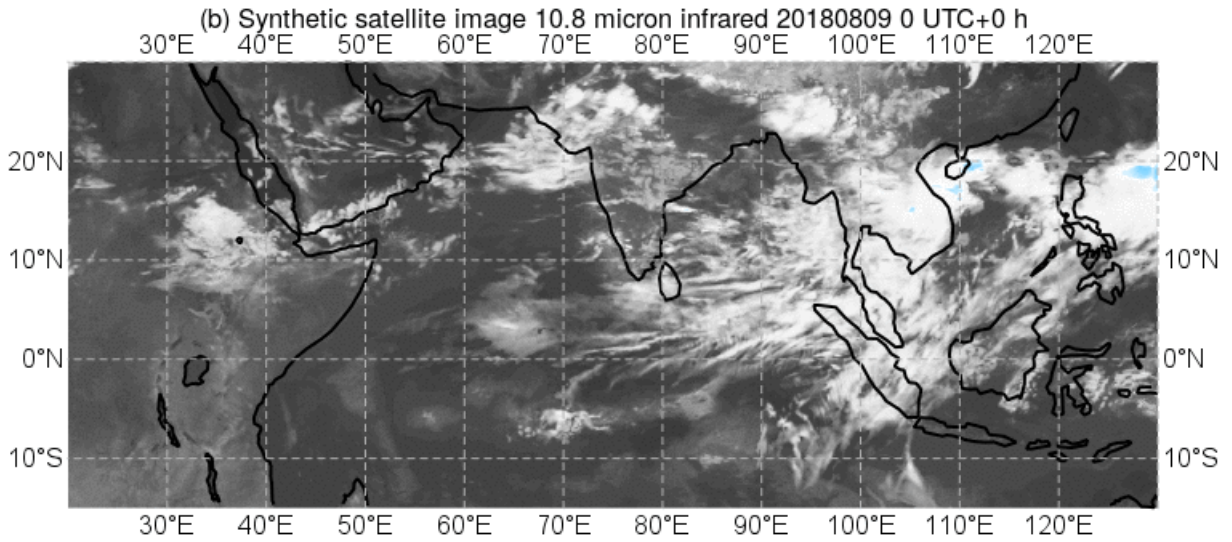

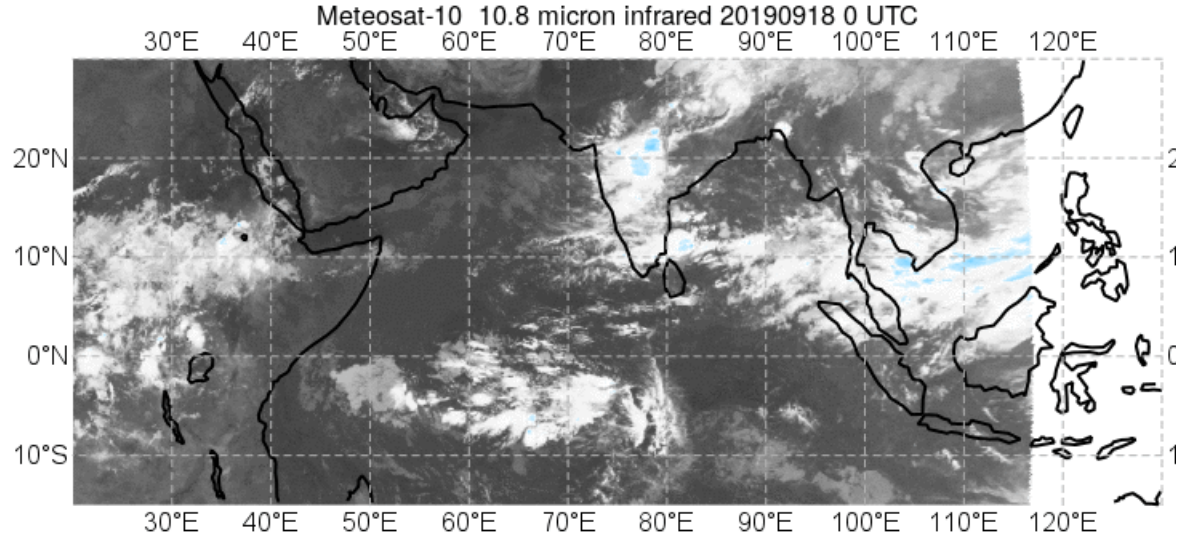

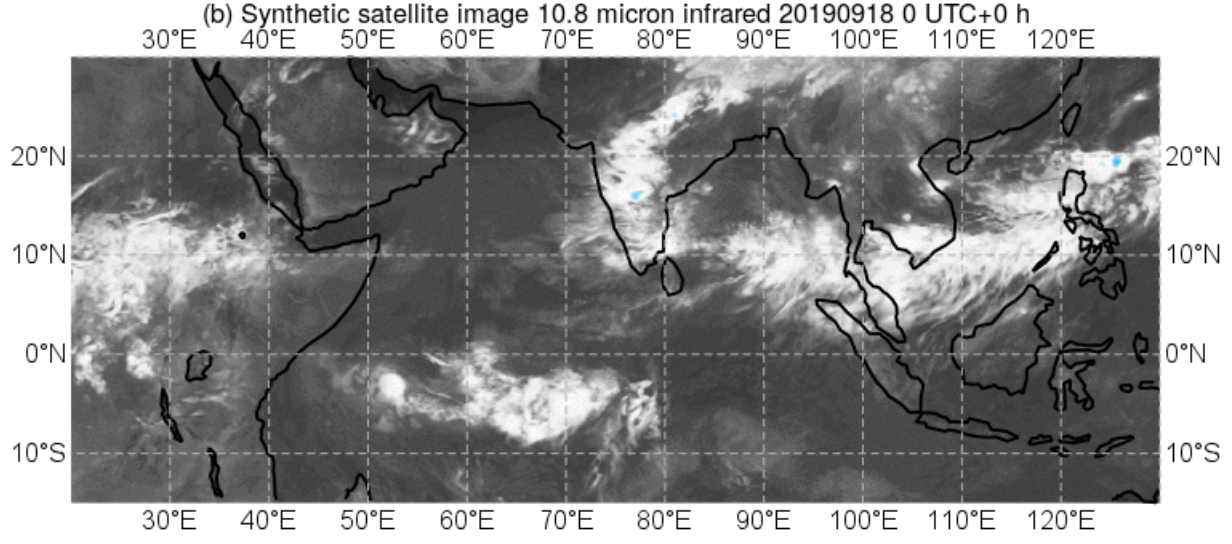

Wavenumber frequency spectra: NOAA and IFS climate

NOAA

IFS

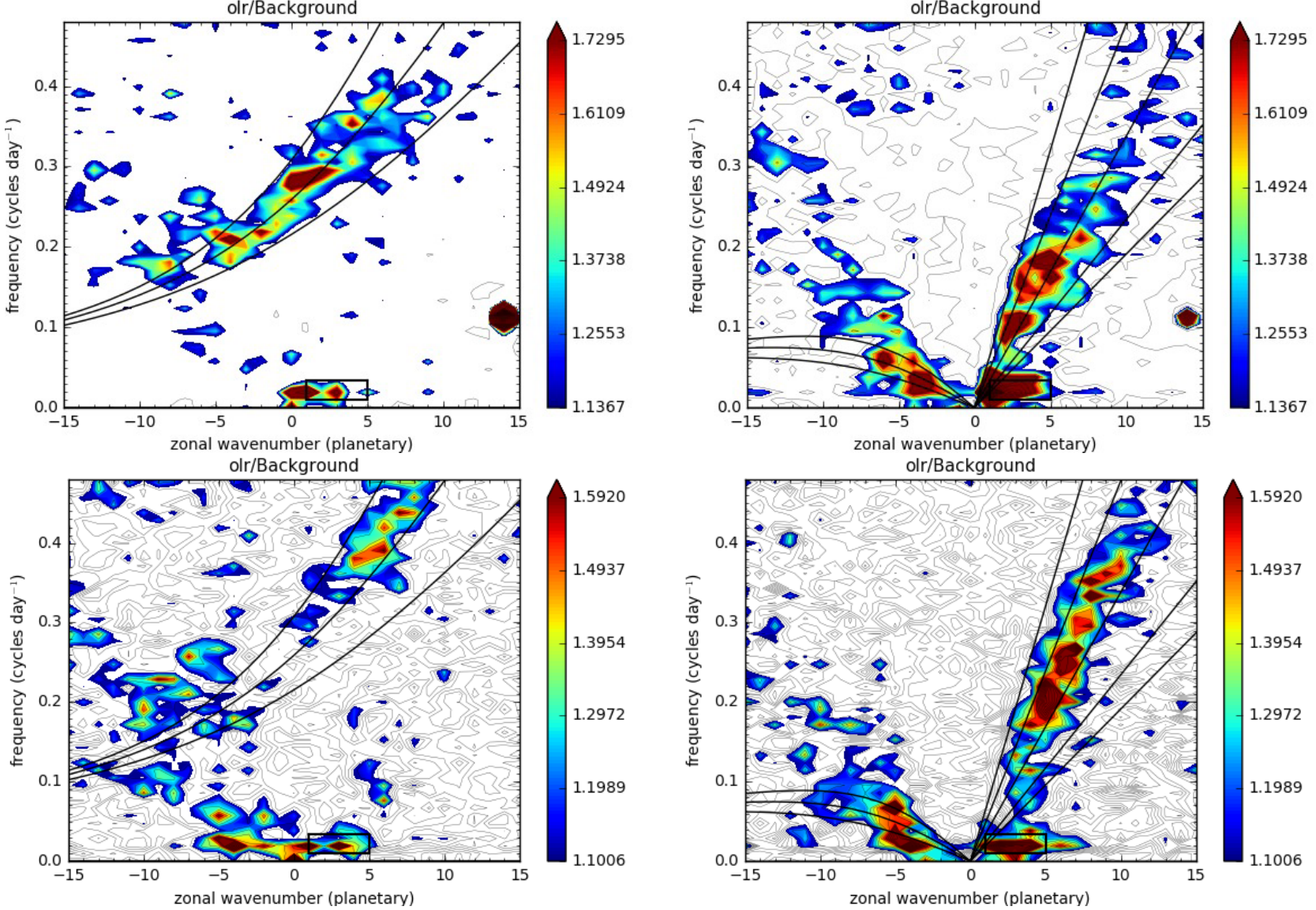

Figure. Wavenumber-frequency diagrams of anomalies of daily data of outgoing longwave radiation from NOAA and from multi-annual coupled integrations with the IFS. The spectra have been averaged over the ±15° tropical band and divided by their background values. Left column: anti-symmetric, right column symmetric component

IR Brightness temperatures and Rossby wave filtered OLR: Aug 9-16 2018 (Kerala floods) and Sept 18-23 2019

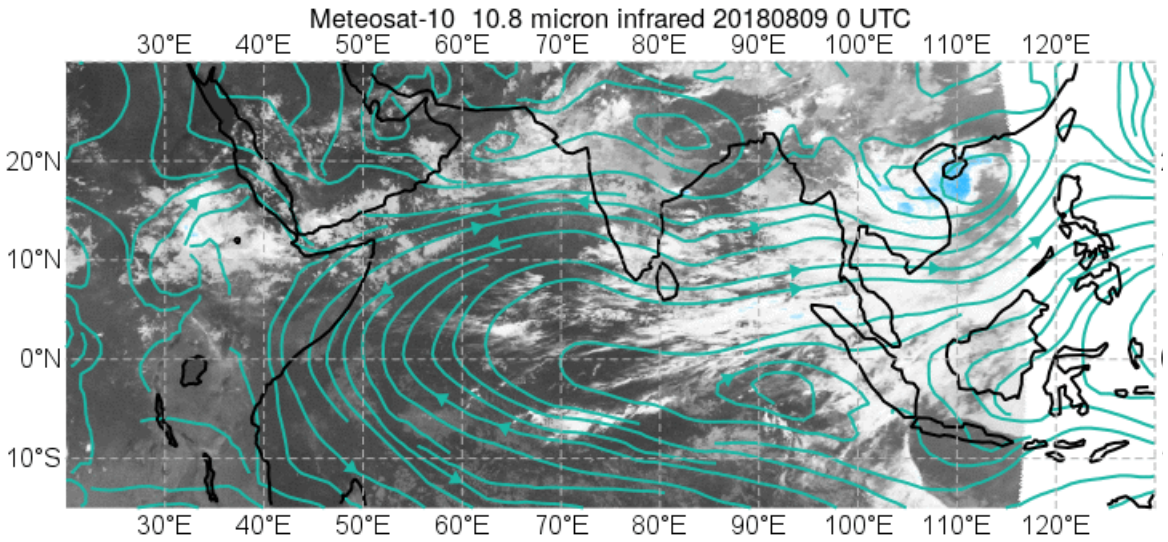

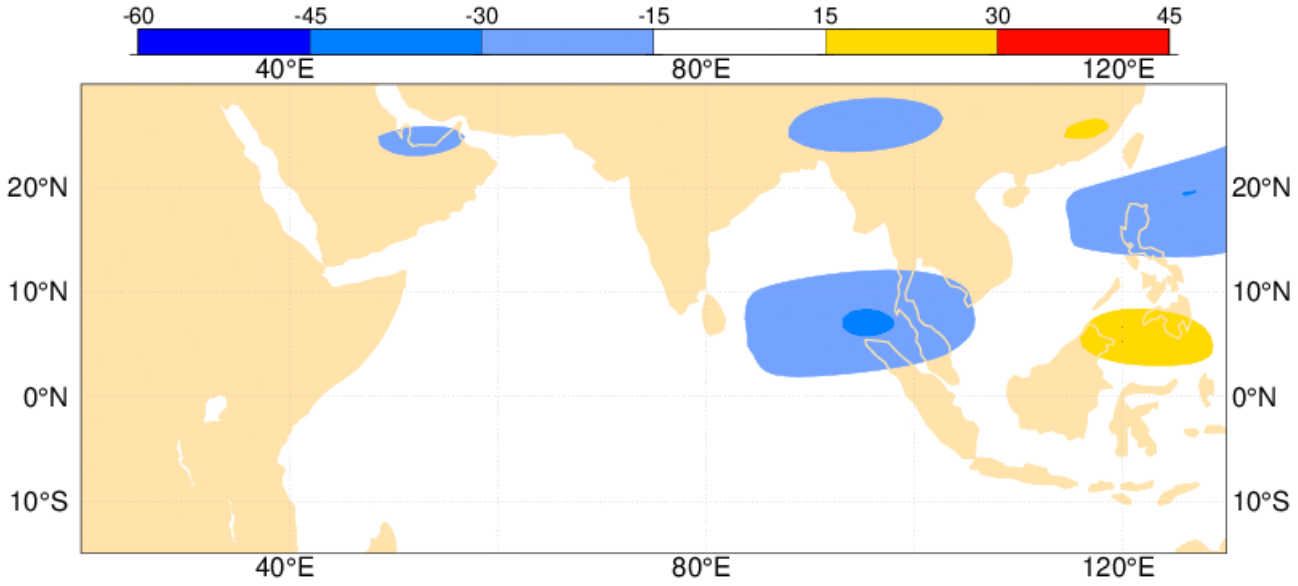

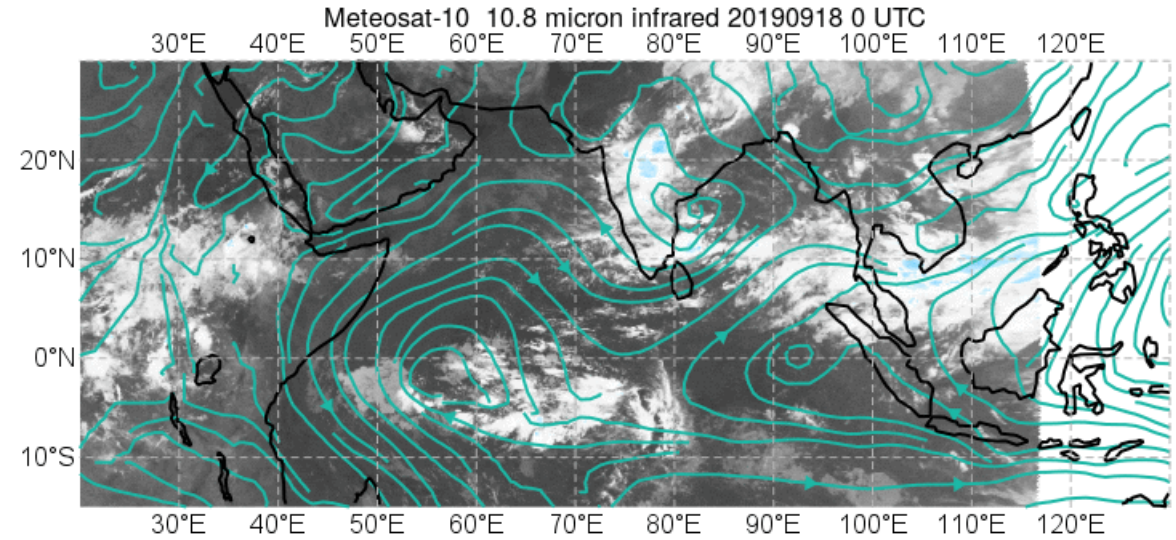

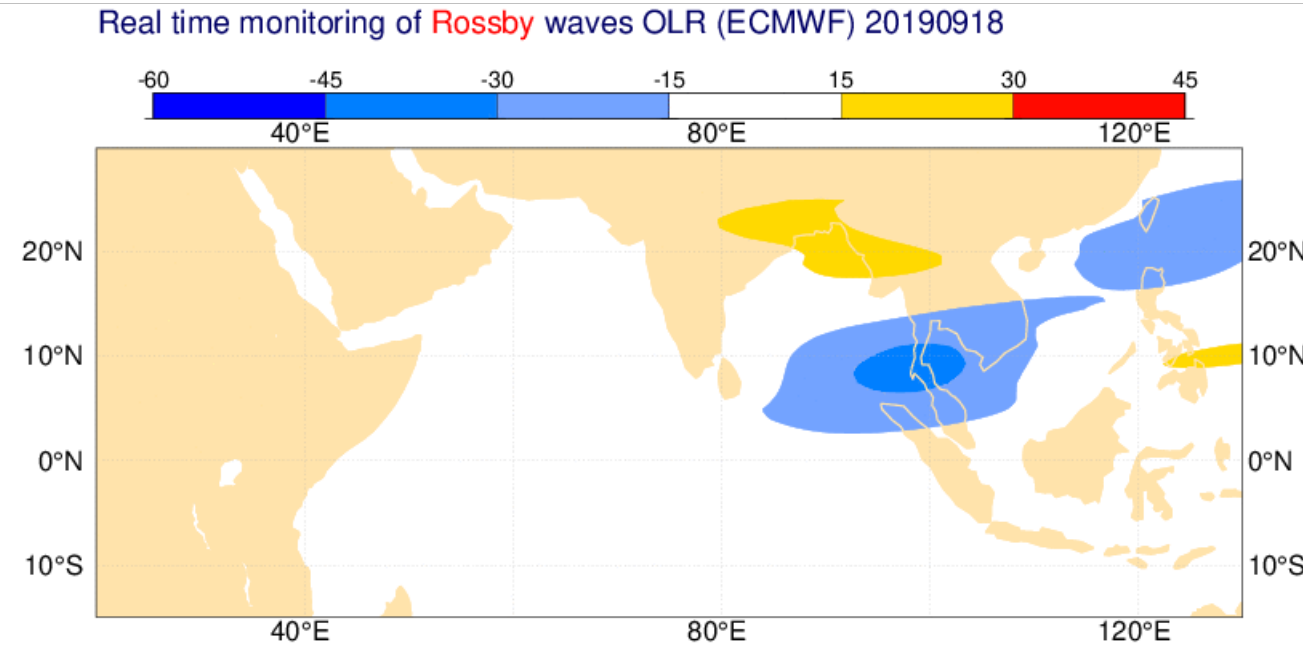

“Kerala”7-8 August 2018 conv+total precipitation: ensemble forecast and Obs

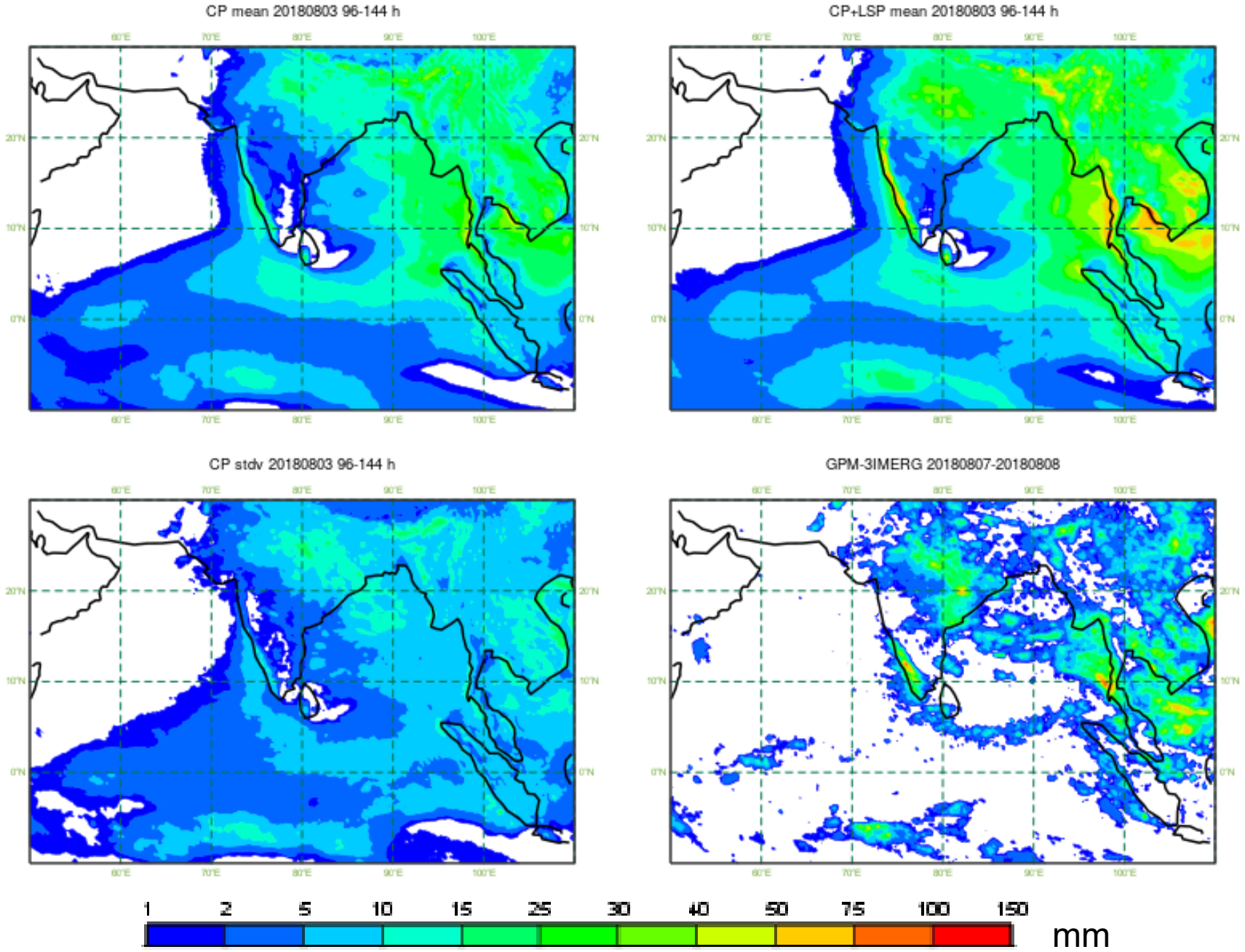

“Kerala”14-15 August 2018 conv+total precipitation: ensemble forecast and Obs

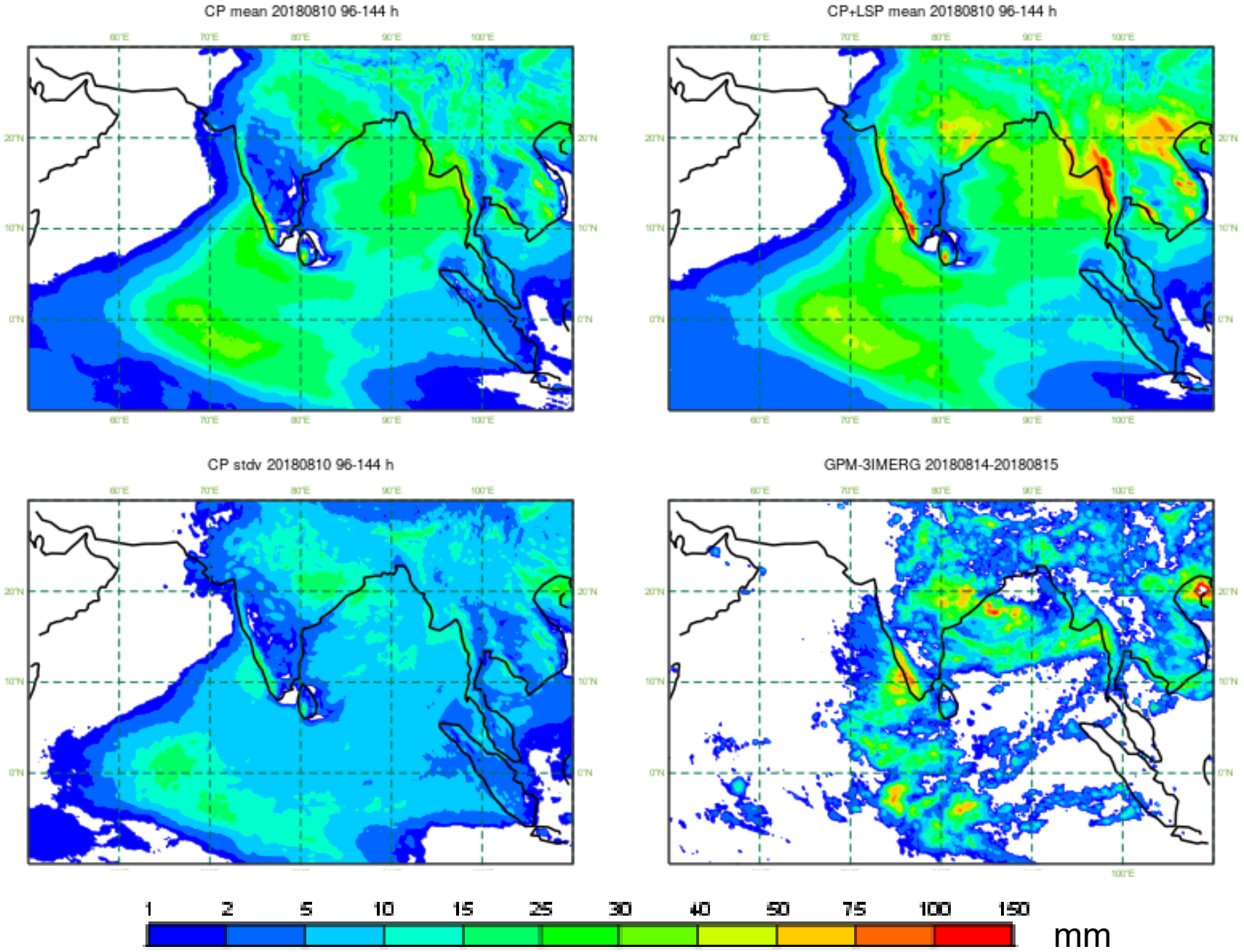

Same but for 21-22 September 2019

CP mean 20190918 96-144

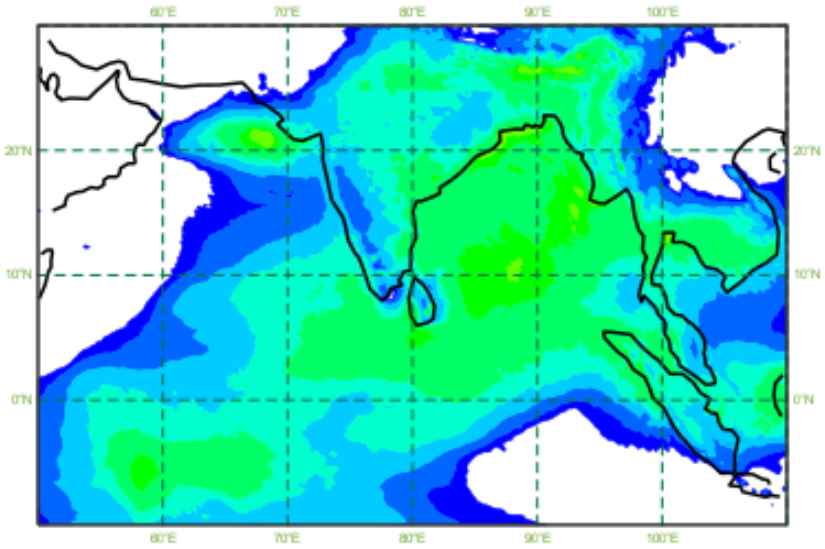

CP+LSP mean 20190918 96-144

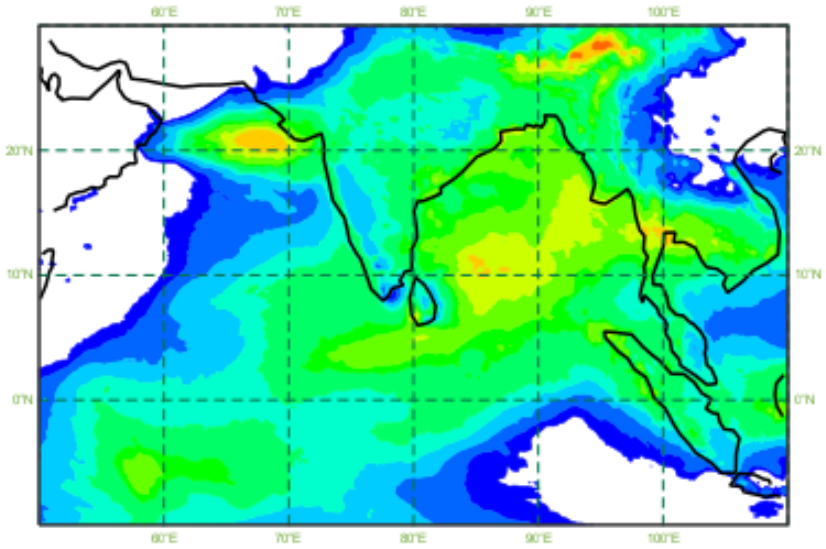

CP stdv 20190918 96-144

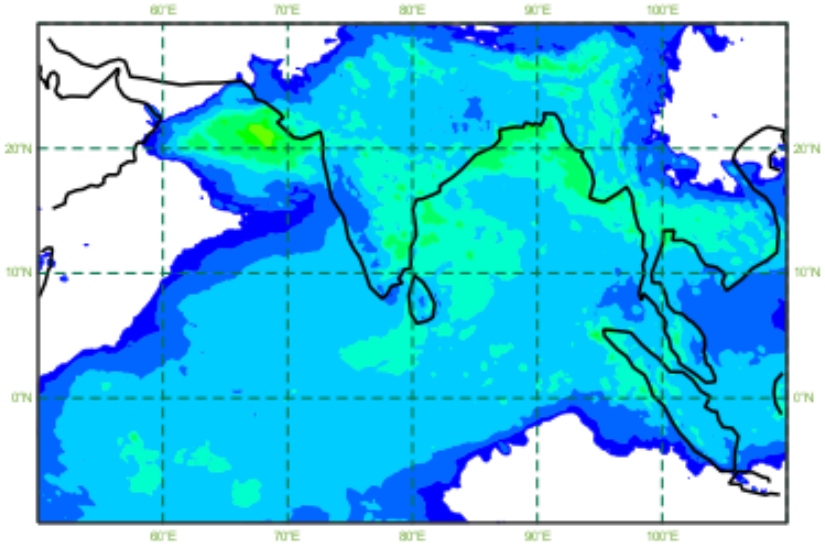

CP+LSP stdv 20190918 96-144

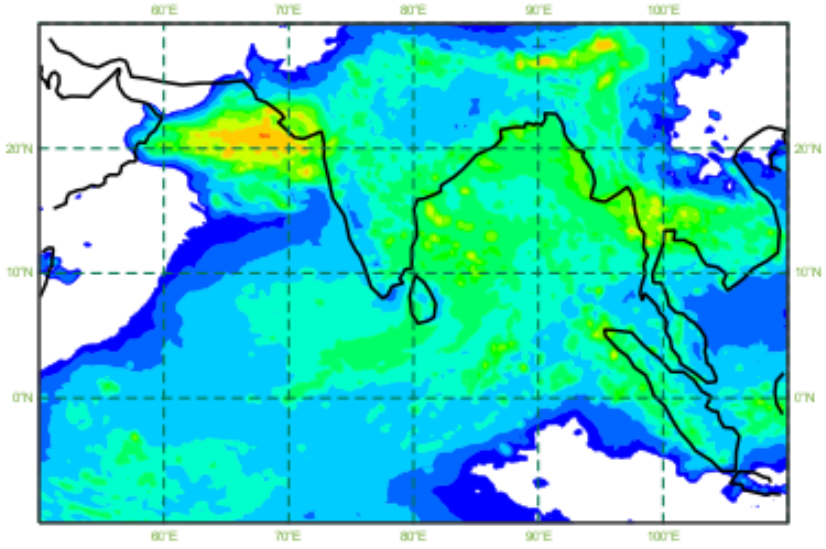

Coherence Spectra as a tool to discern convection (scheme) impact

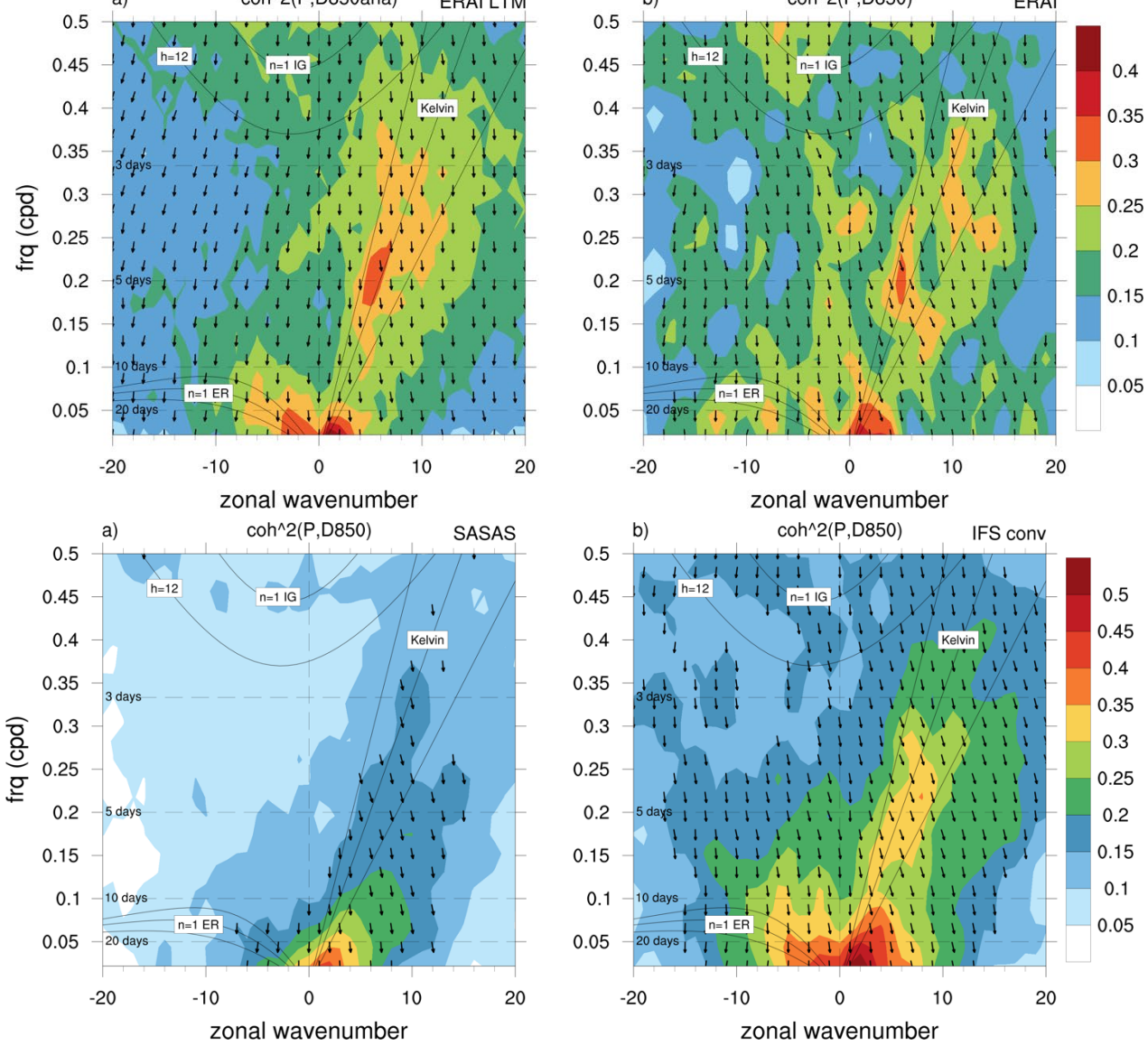

L. Bengtsson et al. (2019) MWR, to appear

Figure. Frequency-wavenumber coherence-squared spectra averaged from 15°S to 15°N between 850hPa divergence and precipitation for a) ERAI JFM long term mean, and b) ERAI valid at the same dates as the 90 day FV3 forecasts with IFS and GFS convection schemes . Phase angles are shown where the coherence-squared is significant at the 95% level.

Hovmöller Diagrams of Microwave first-guess fits

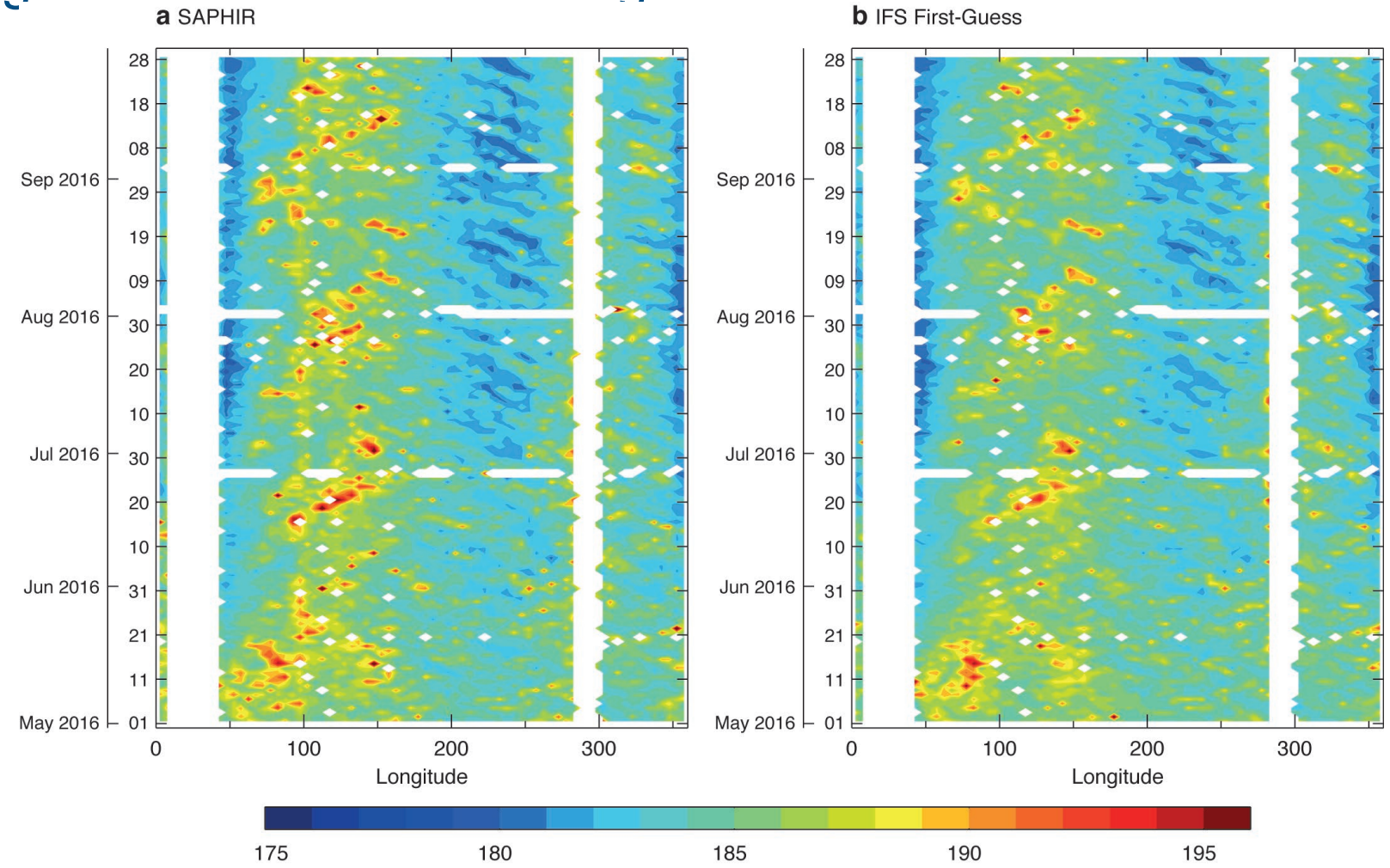

Figure. Hovmöller diagrams (longitude versus time) of the microwave brightness temperatures (K) averaged over the tropical belt from May to September 2016 as obtained from the passive microwave sounder SAPHIR instrument developed by the French space agency CNES and from the first-guess (background) forecasts of the IFS. Figure courtesy Alan Geer, ECMWF.

MJO events and apparent heating rates Q1 and Q2 during DYNAMO

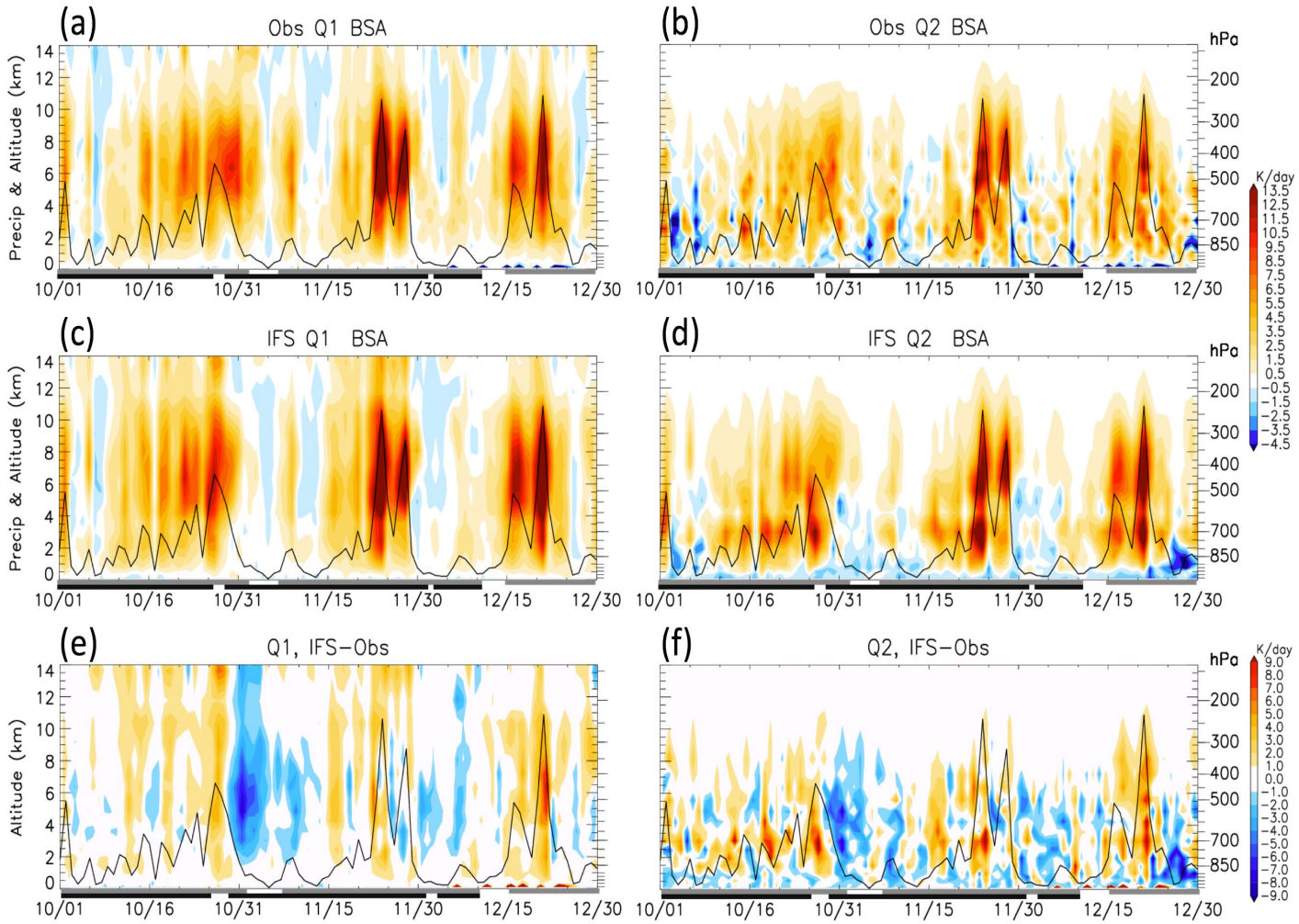

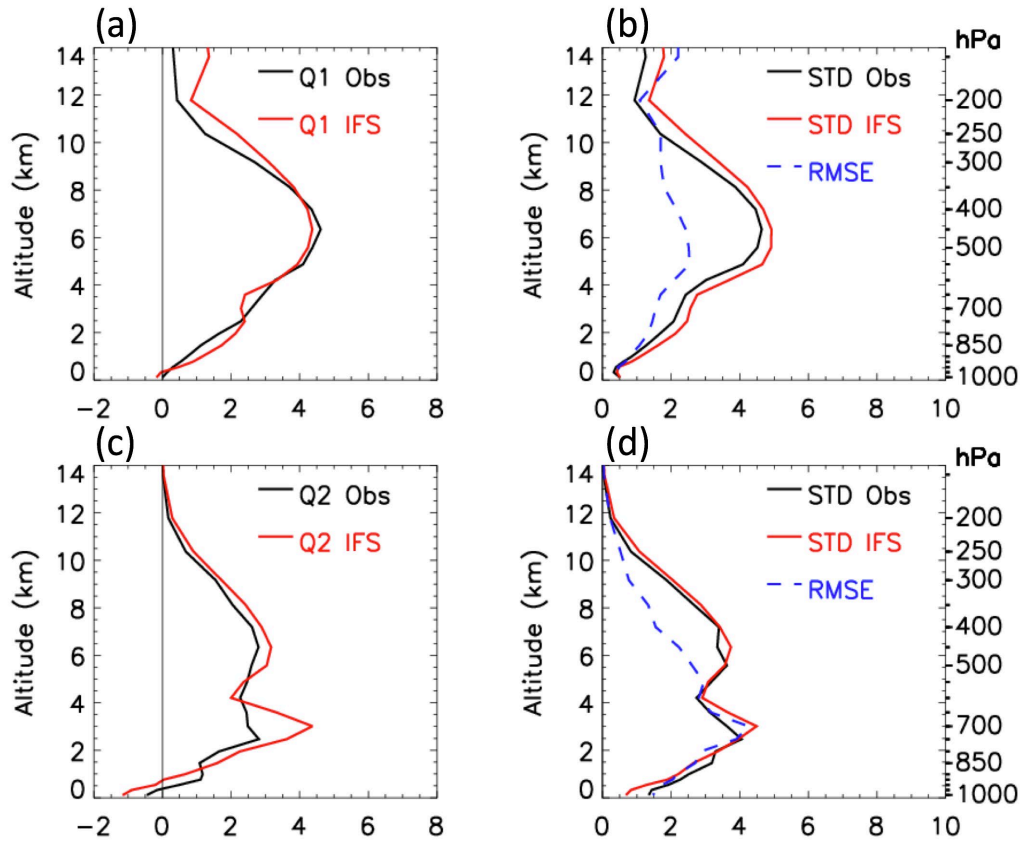

J.-E Kim et al. 2017, JAS

Figure. Time series of apperent heating and moistening rates from radiosonde budgets and IFS day 2 integrations over the DYNAMO campaign area during October-December 2011.

Kelvin waves vertical T-anomalies Obs and mode'

At z~10 km, warm anomaly and convective heating are in phase, leading to :

- the conversion of potential in kinetic energy = αω
- The generation of potential energy = N Q

M. Herman et al. JAS 2016

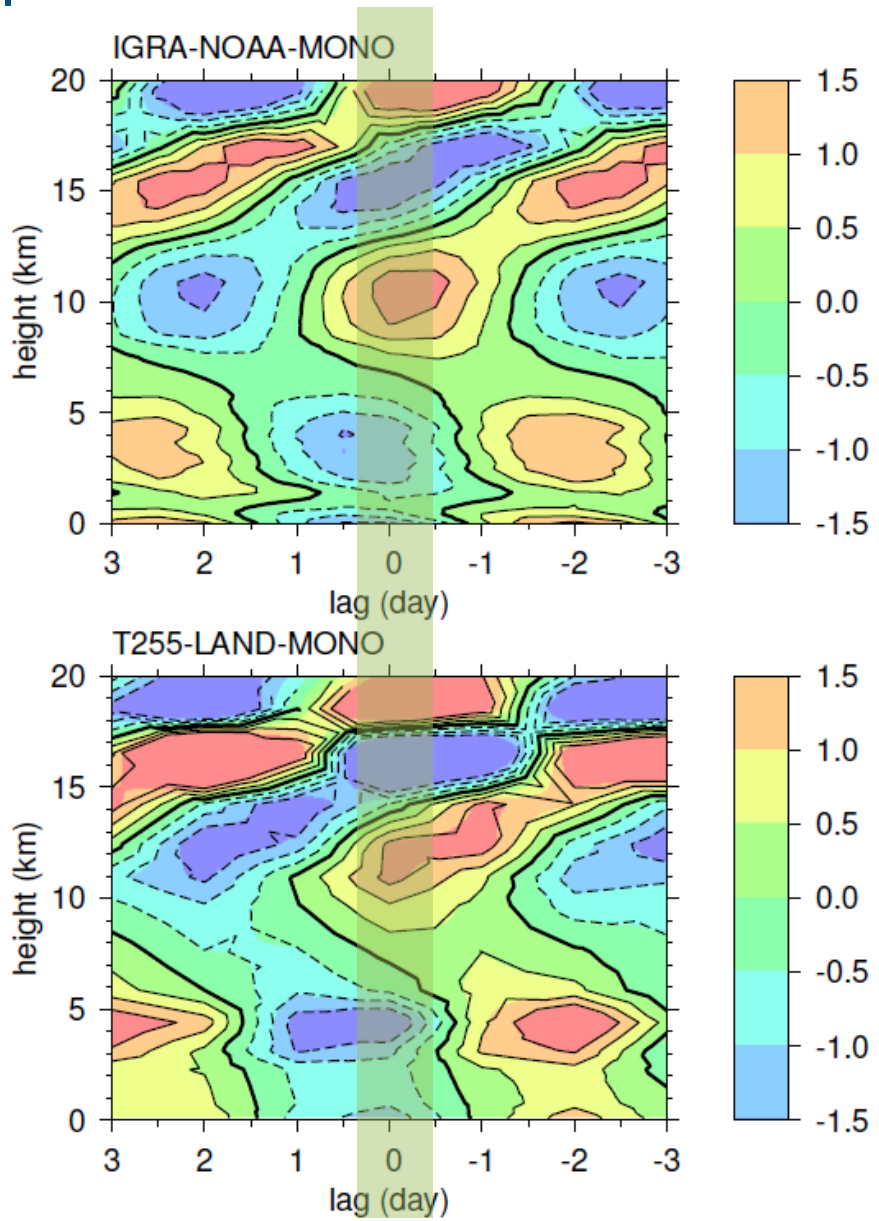

Kelvin waves vertical T-anomalies in equatorial b-plane model with dx=2.5 km

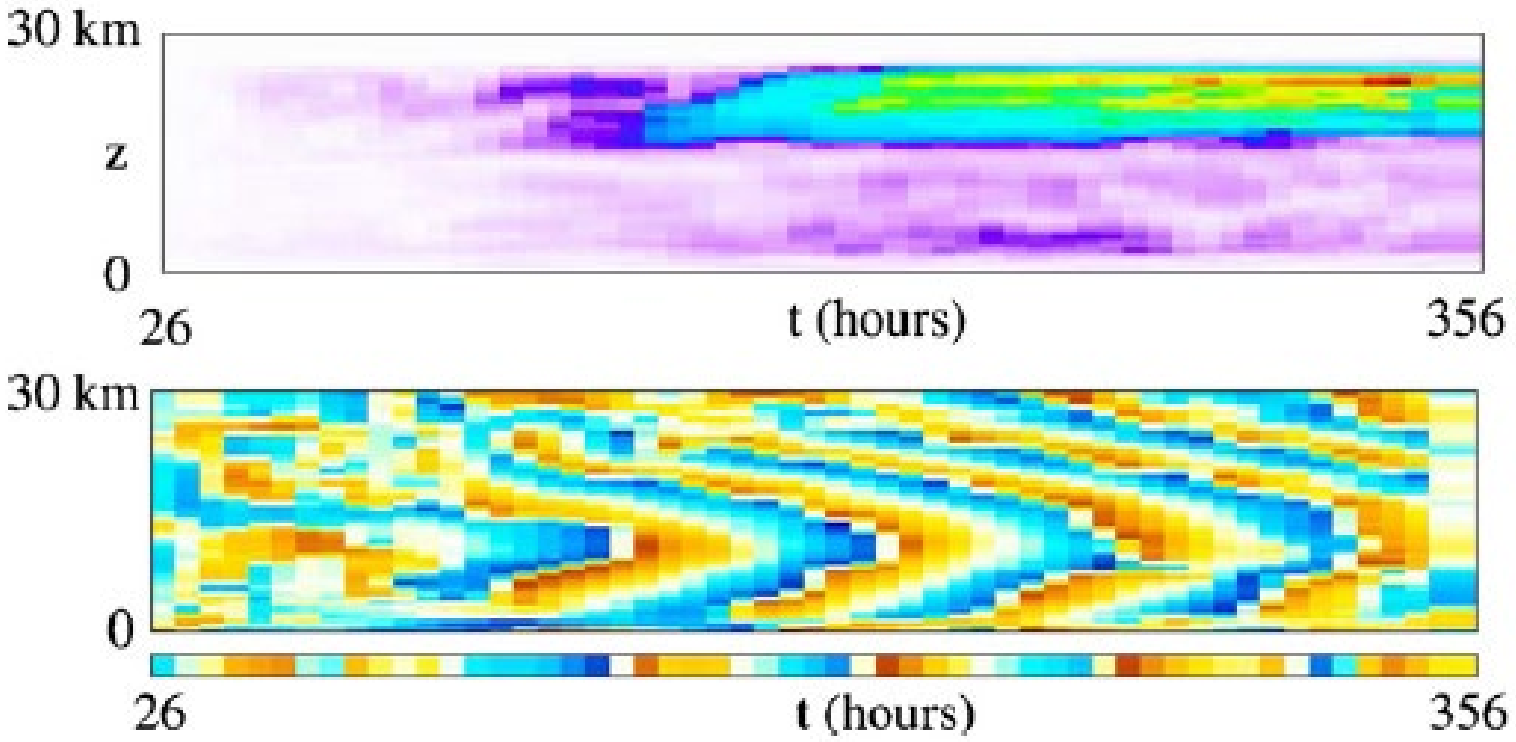

Figure 9. Time-height section of the amplitude (above) and phase (below) of wavenumber 10 in the *Θ'* field. The horizontal strip below the phase plot shows the phase of the surface rain rate. Units: K_{-1} for the amplitude and degrees for the phase.

from G. Shutts (2008, Dyn. Atmos. Oc.)

And the others …….?

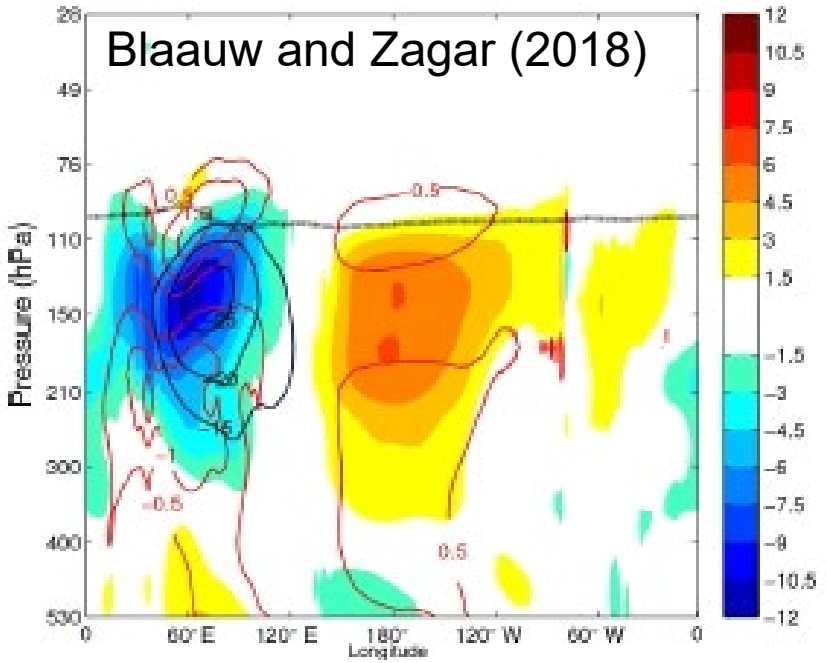

Kelvin U anomaly JJA

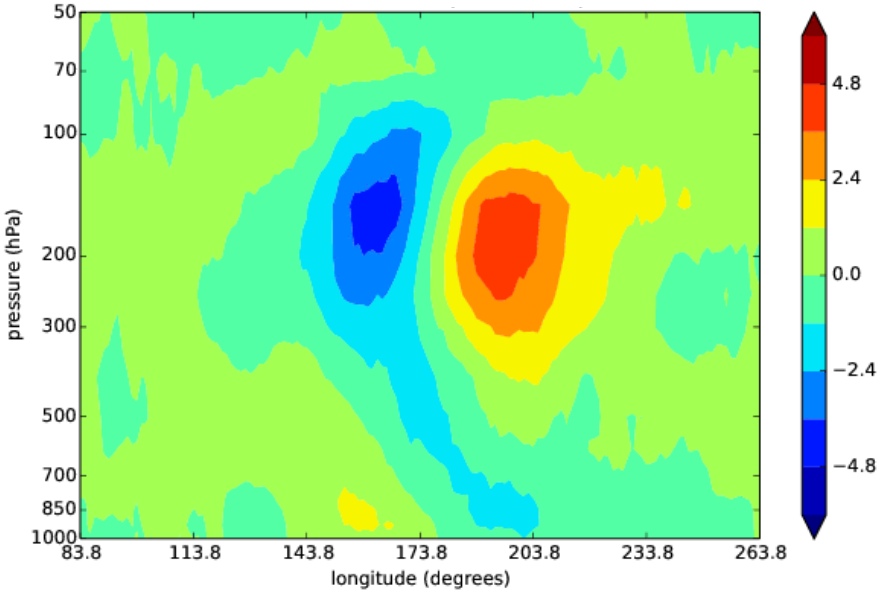

MJO U anomaly DJF

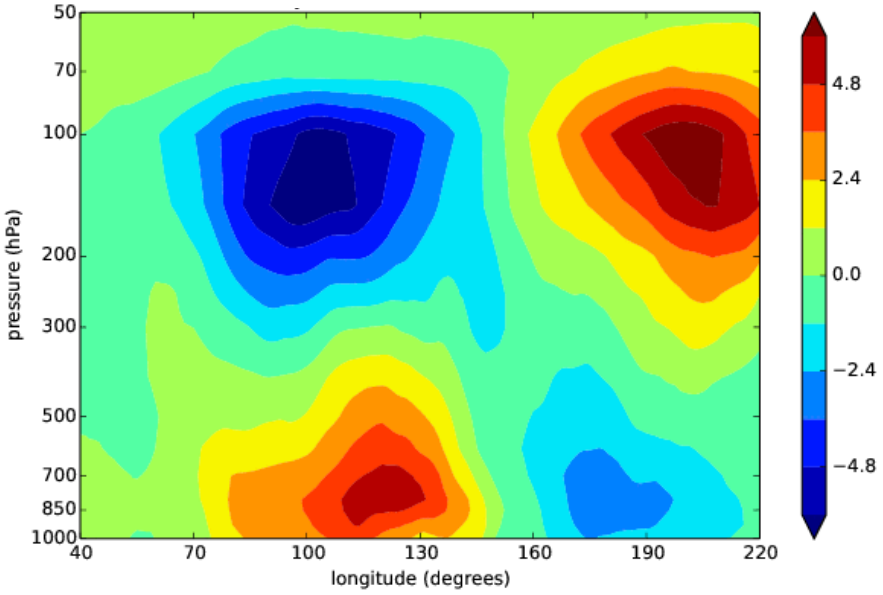

Rossby U anomaly JJA

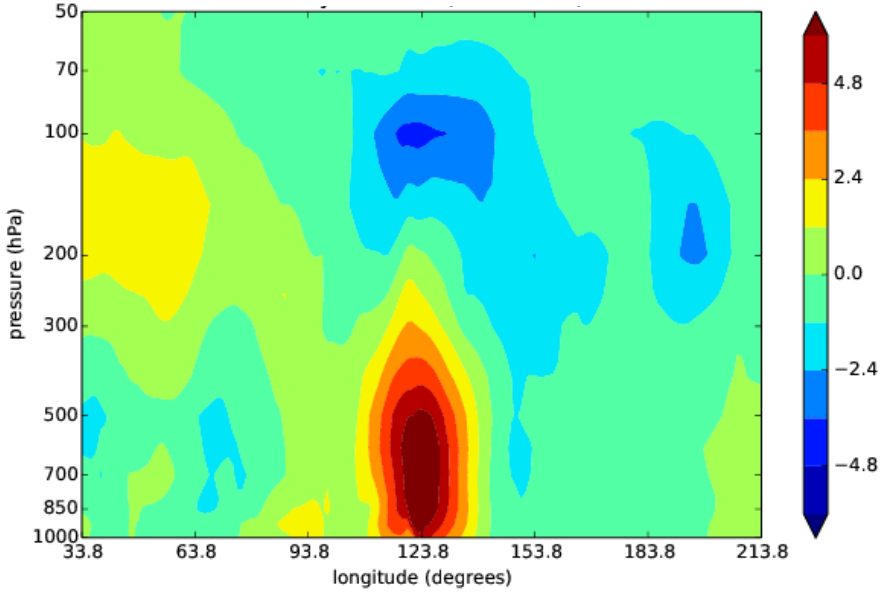

“Predictability” of Kelvin and Rossby waves

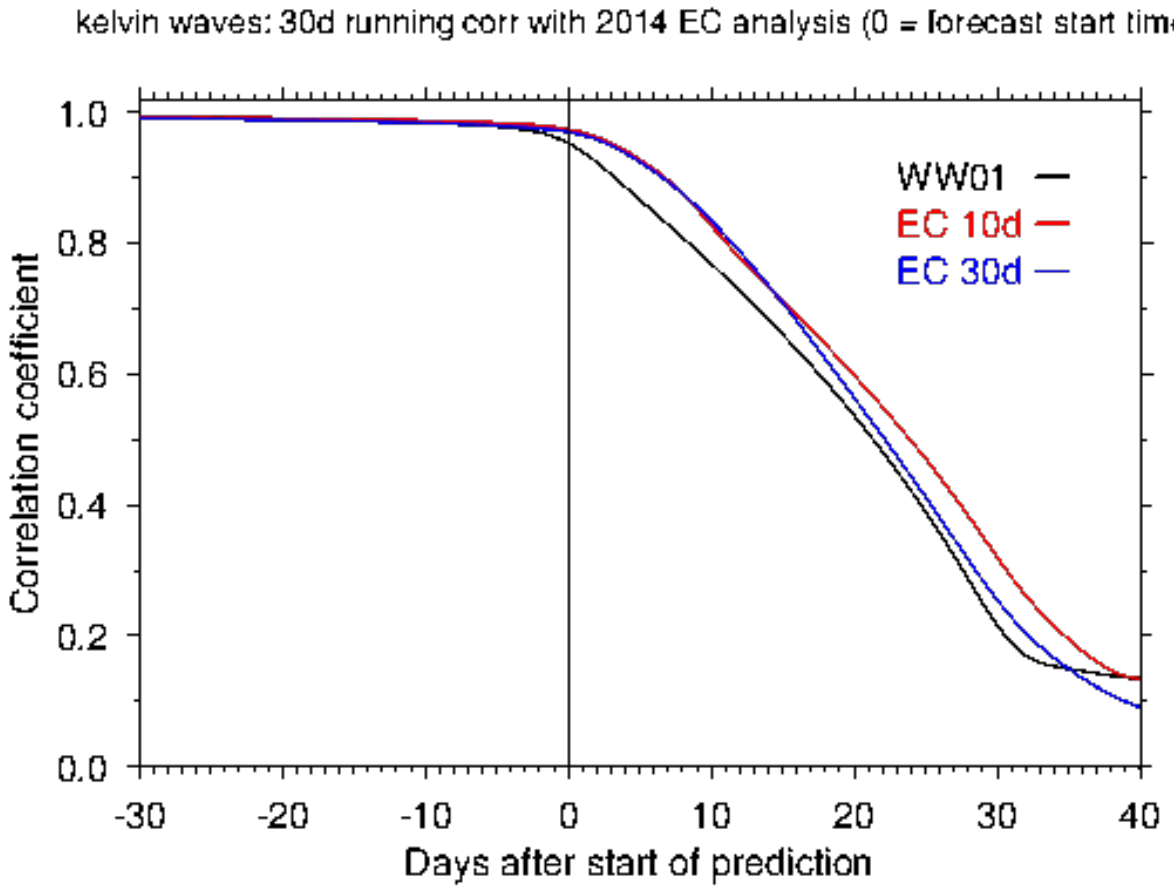

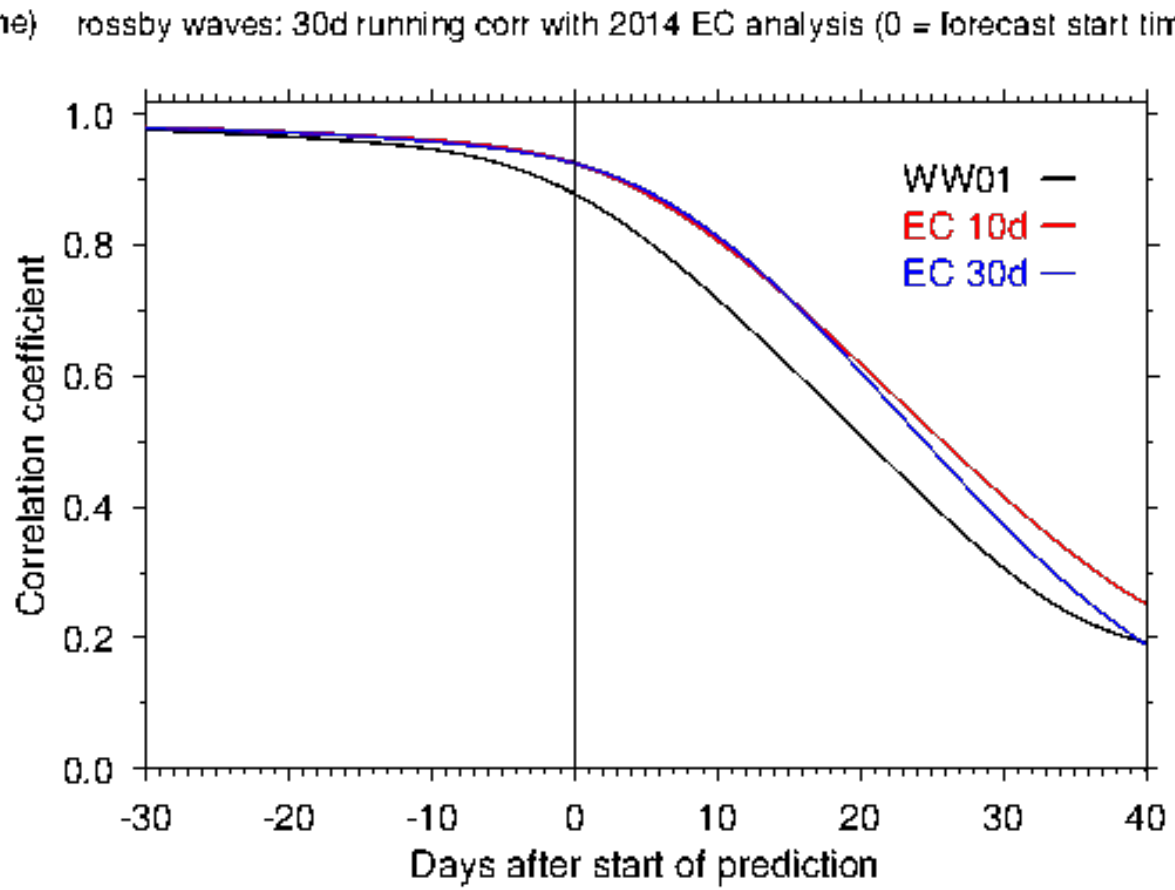

Skill of MJO predictions over time at ECMWF and compared to other Centers

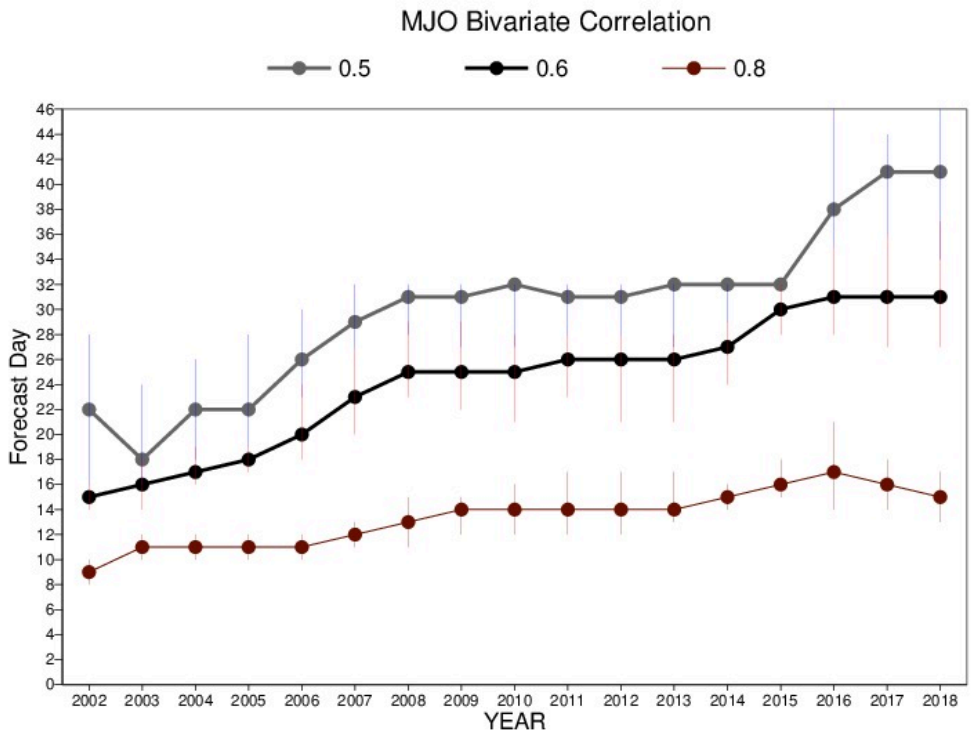

Figure. Evolution of the skill of the IFS 11-member 30-year reforecasts of the MJO for different thresholds of the correlation coefficient between the forecast Wheeler and Hendon MJO index. Courtesy Frederic Vitart, ECMWF

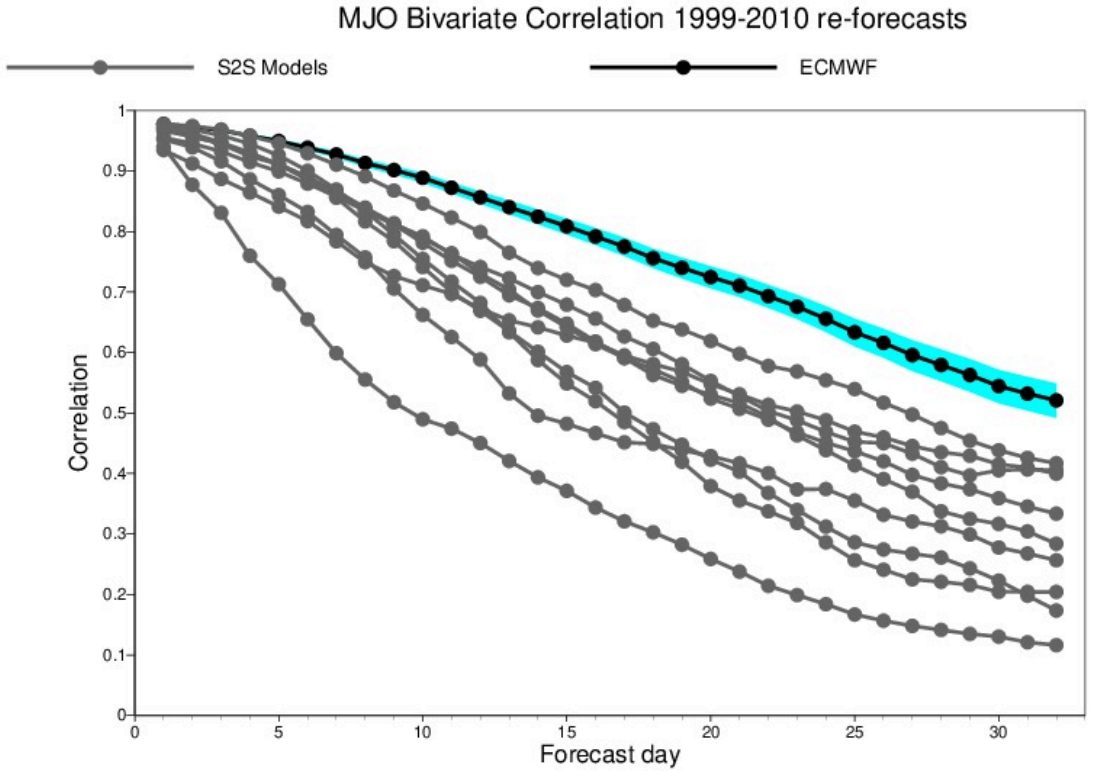

Figure. Same but comparing the correlation between the observed MJO anomalies and those produced by the IFS reforecasts for 1999-2010 (black line) to those of the other global prediction systems in the S2S database (grey lines).

Global spectra of Rot & Div at 250 hPa for different resolutions

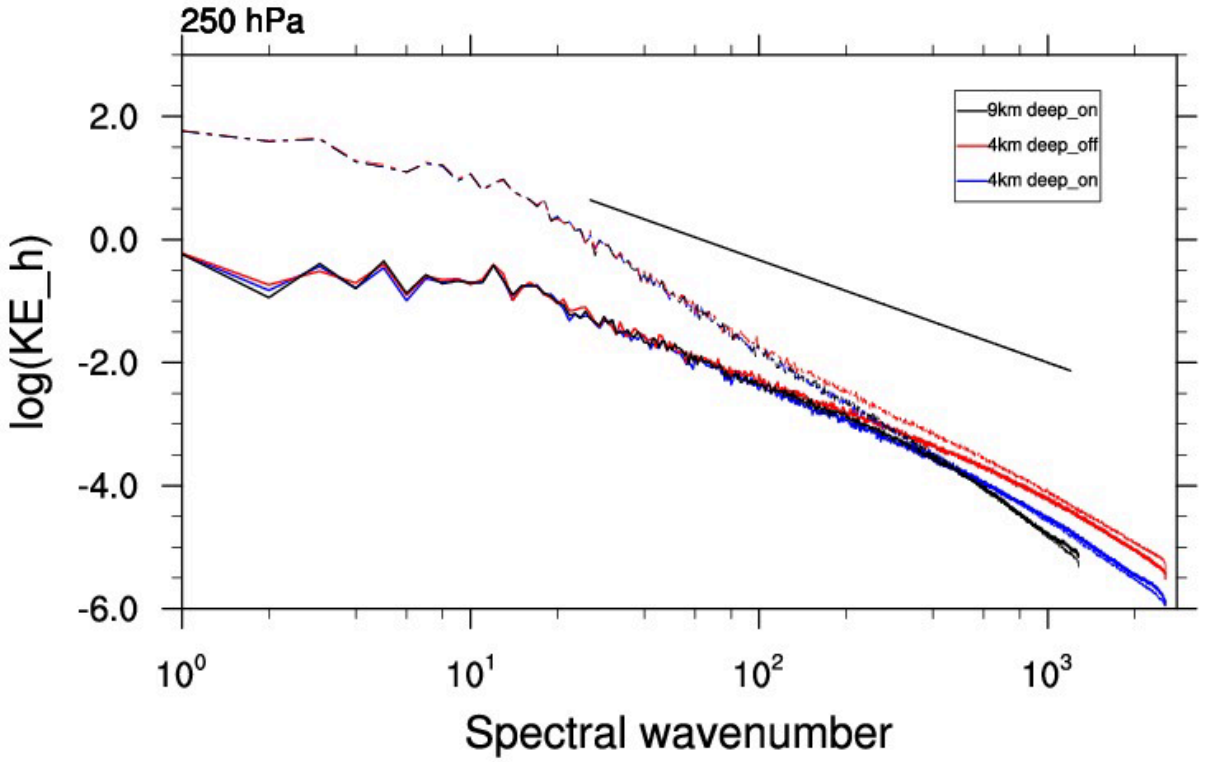

Figure . Gllobal spectra of the rotational (dashed) and divergent part (solid) of the horizontal kinetic energy at 250 hPa as a function of the global wavenumber for different model configurations: 9 and 4 km horizontal resolutions with the deep convection scheme and 4 km without the deep convection scheme. The straight black line denotes the -5/3 spectral slope.

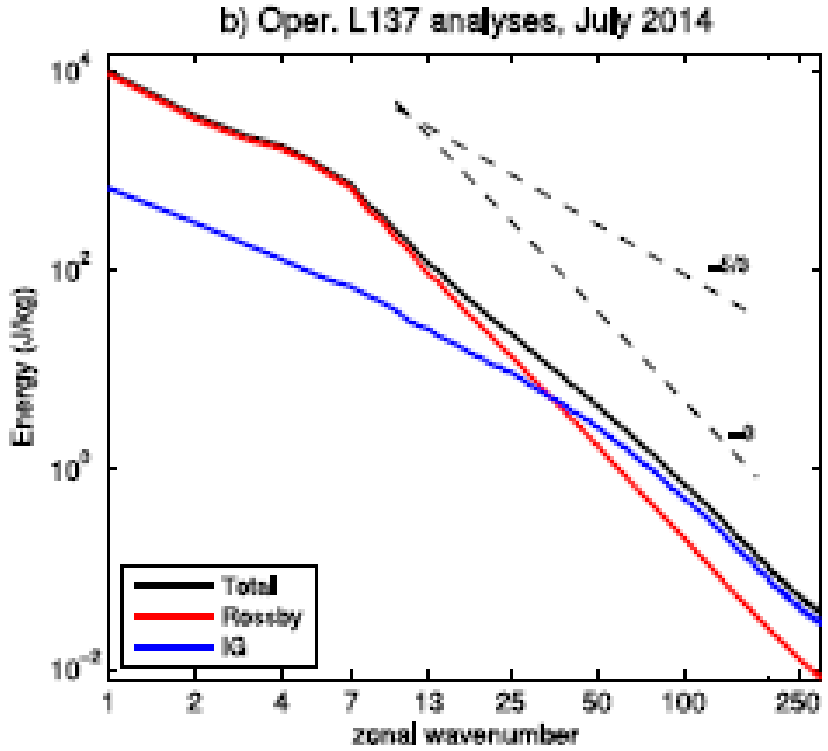

Figure . Extract from Žagar et al. JAS 2017 using ECMWF analyses from July 2017 and a decomposition into Rossby and IG modes using MODES. Integration is over all meridional and vertical modes

Scale dependent APE-KE Analysis

from S. Malardel and N. Wedi (JGR 2016)

following Augier and Lindborg (2013)

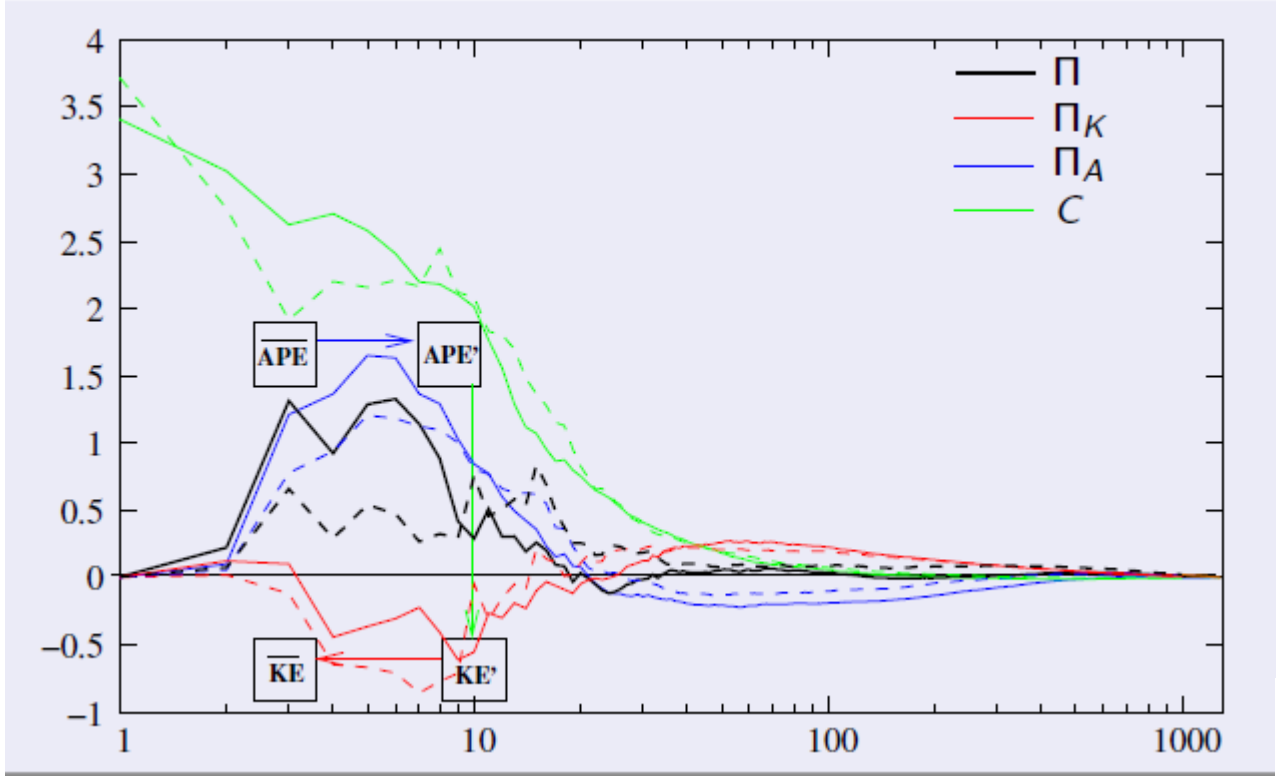

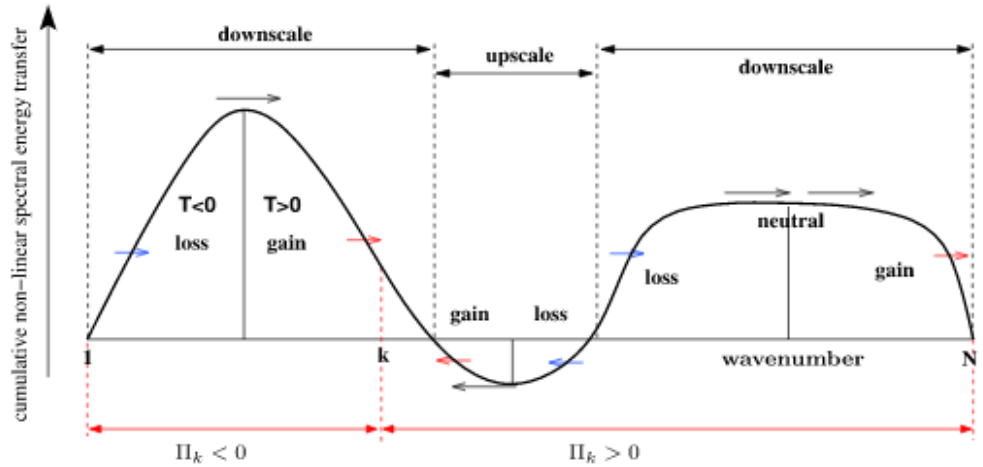

Figure 3. Schematic graph of cumulative nonlinear spectral energy flux Π. Downscale transfer is given for $\Pi > 0$ and upscale transfer for $\Pi < 0$. See text for a more detailed explanation.

$$\partial_t E_{K\,l} = C_l + T_{Kl} + L_l + F^{p_b}_{K\,l} - F^{p_t}_{K\,l} - D_{Kl}$$

$$\partial_t E_{Al} = -C_l + T_{Al} + F^{p_b}_{A\,l} - F^{p_t}_{A\,l} + G_l - D_{Al}$$

$$\Pi_{(K,A)\,l} = \sum_{l \le j \le N} T_{(K,A)\,j},$$

Energy transfer in mesoscale convective systems

from Y. Sun, R. Rotunno, F. Zhang
J. Atmos. Sci. 2017

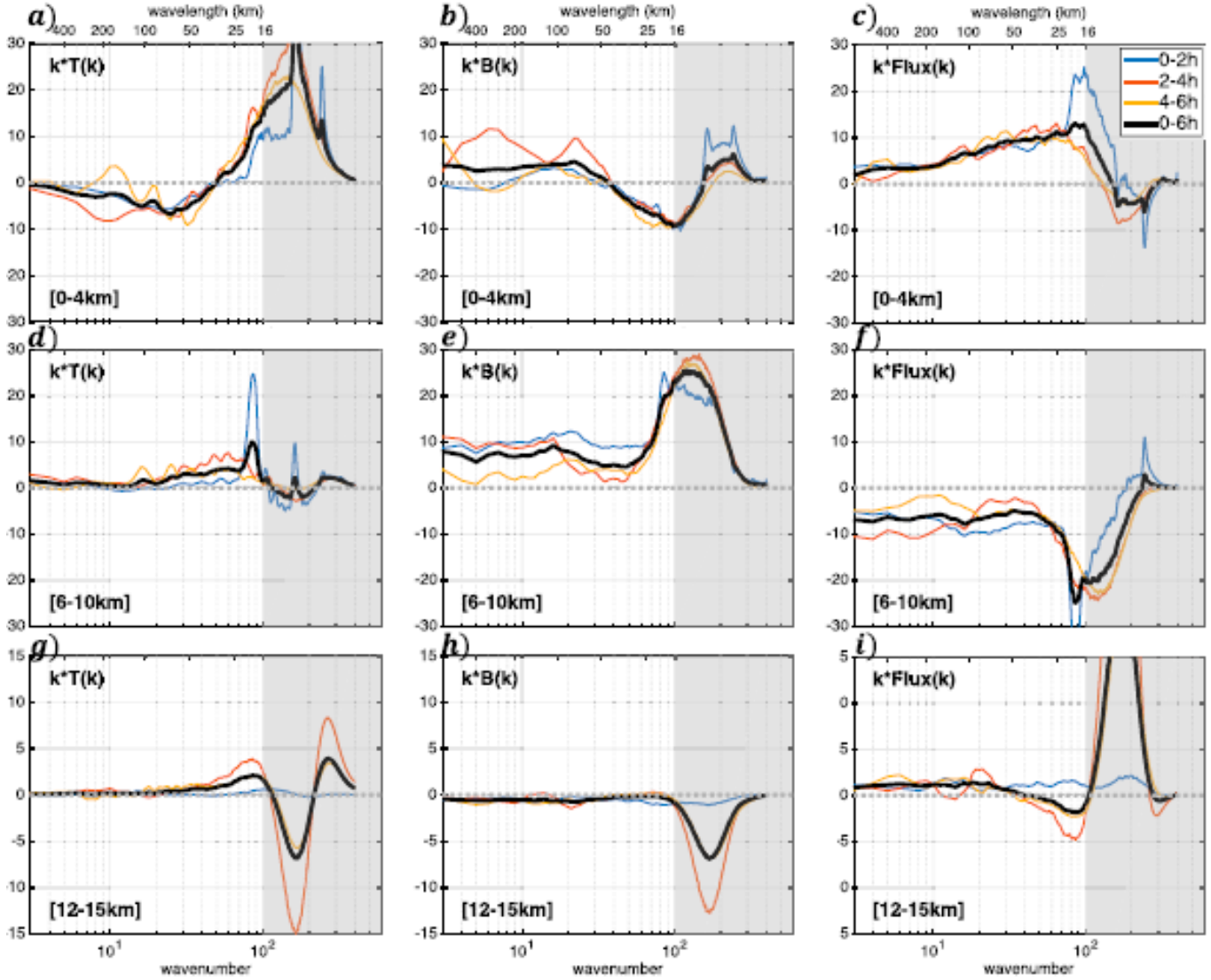

B=buoyancy flux=**C**onversion

Fig. 9 Kinetic energy spectrum analysis (10^{-6} m^2s^{-3} kg m^{-3}) at different height levels

Mesoscale convective systems, their propagation and the diurnal cycle

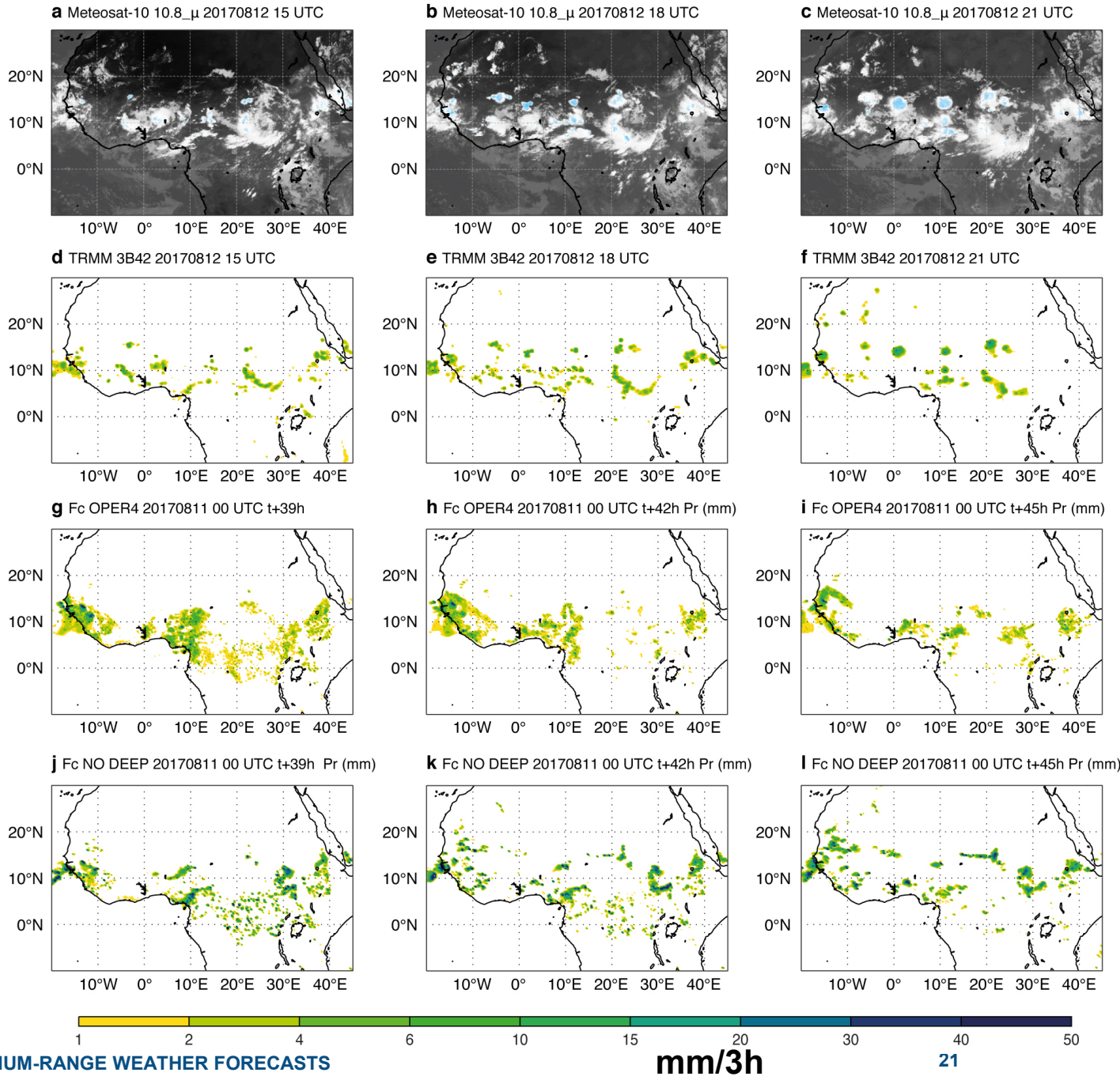

Figure: Sequence of Meteosat 10 infrared and TRMM rainfall radar sequences over Sahel and reforecast for **8 Aug 2017** at 4 km with and without deep convection parametrization

Lightning and the diurnal cycle

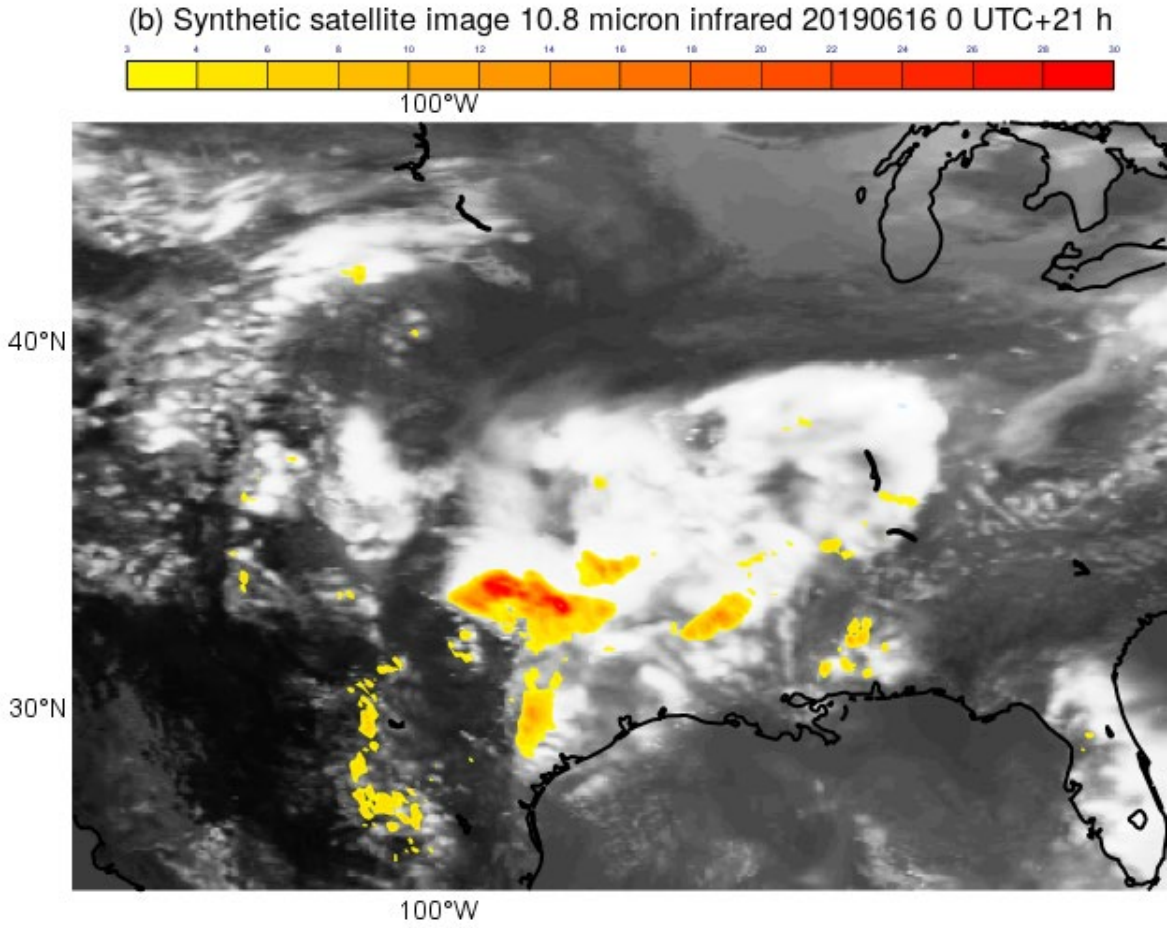

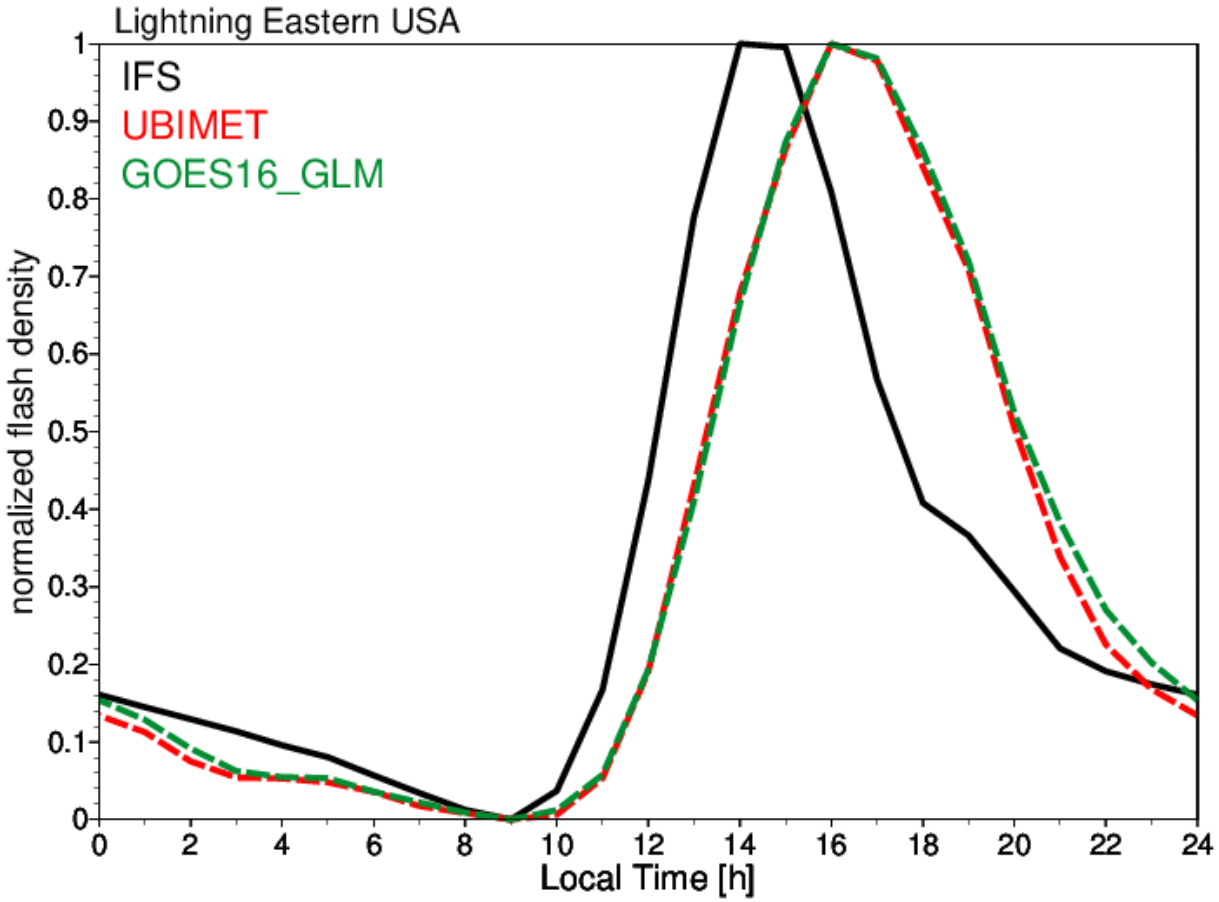

Figure: The lightning product has been developed by **P. Lopez** (MWR 2019) and uses the CAPE, frozen water content and cloud base height from the convection

Ensemble representation SPP

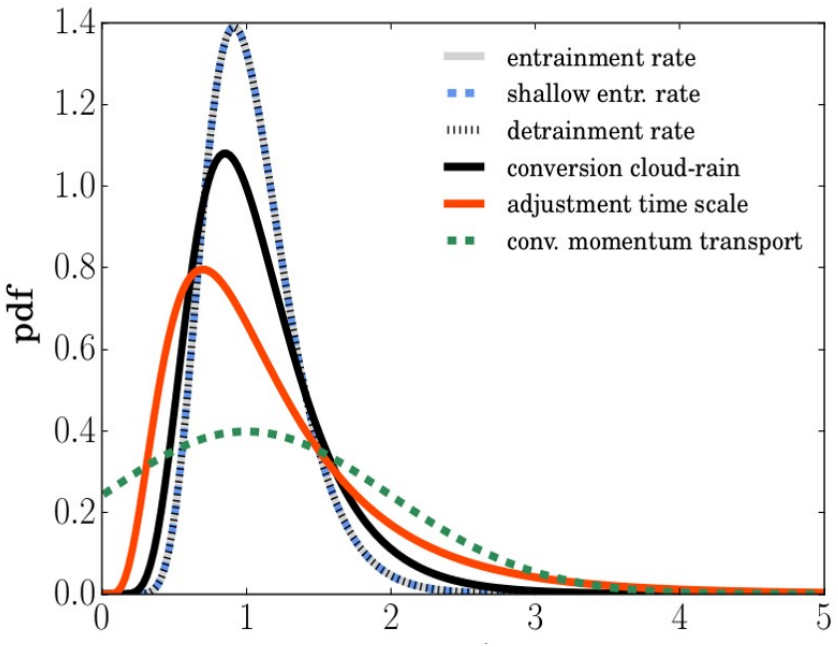

see Ollinaho et al. QJRMS 2017

Figure: Pdf of perturbed convection parameters and standard deviation (spred) of total precipitation during August from 15-member ensemble runs

August 2017

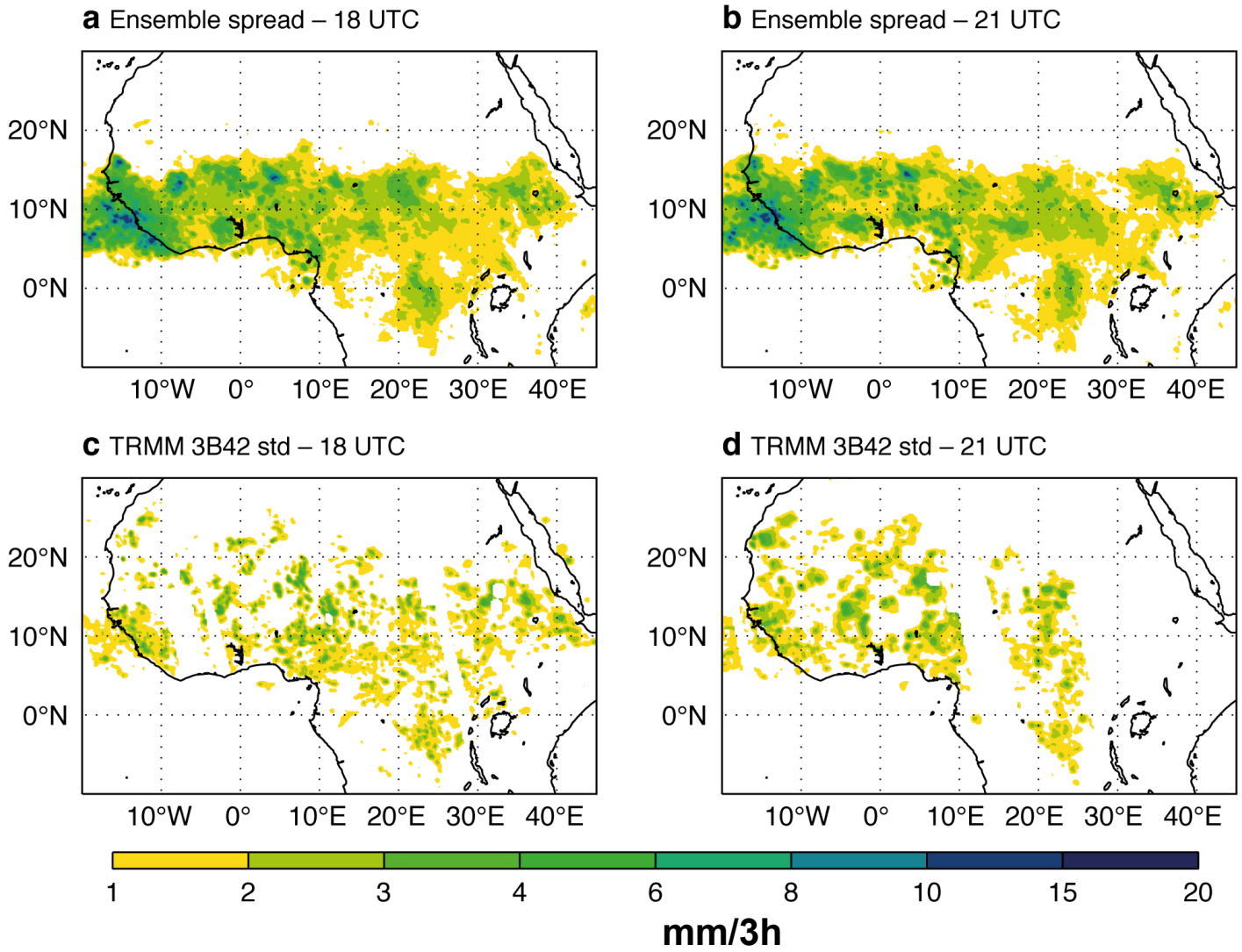

Direct convection-dynamics coupling via mass flux divergence

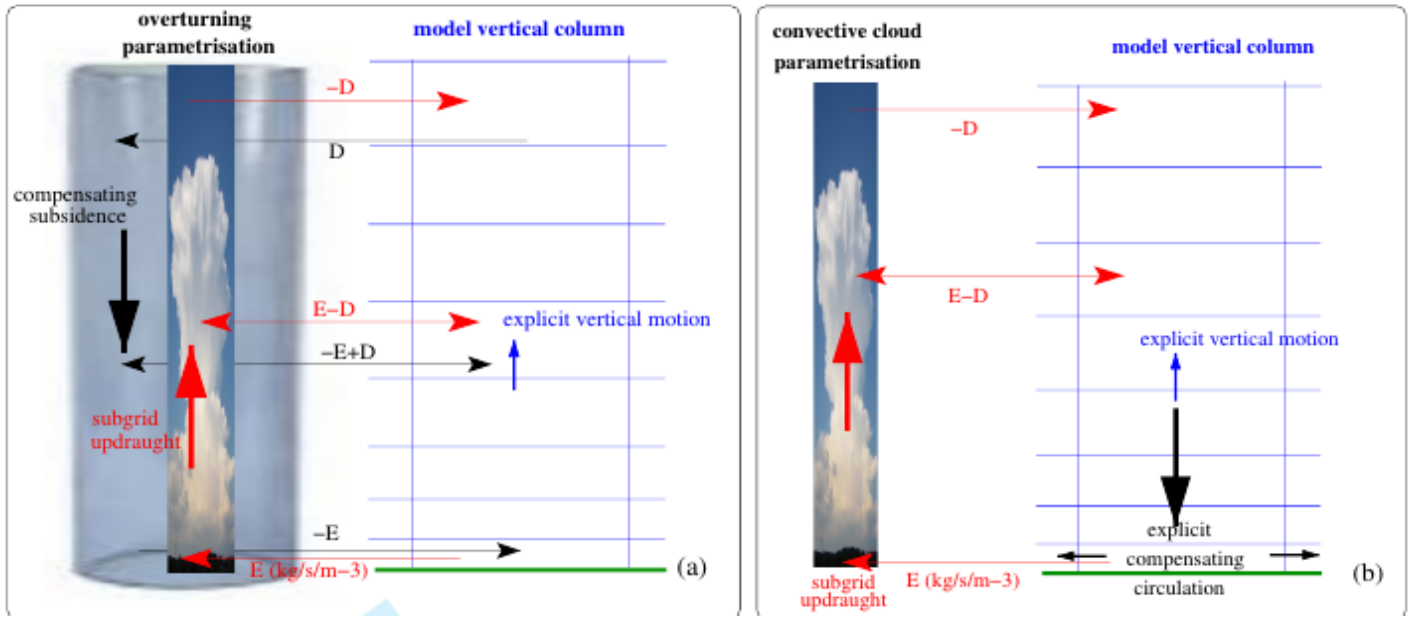

$$\frac{\partial \overline{\rho w' \psi'}}{\partial z} = \frac{\partial \left[\sigma_u \rho w_u \left(1 - \frac{w_e}{w_u} \right) (\psi_u - \overline{\psi}) \right]}{\partial z}$$

$$f(\delta x) = \left(1 - \frac{w_e}{w_u} \right)$$

$$\frac{\partial \overline{\rho}}{\partial t} = -\nabla_h \cdot (\overline{\rho}\, \overline{\mathbf{u}}_h) - \frac{\partial (\overline{\rho}\, \overline{w})}{\partial z} - \frac{\partial M}{\partial z}$$

$$\frac{\mathrm{D}\overline{\psi}}{\mathrm{D}t} = \underbrace{+g \frac{\partial (M \psi_u)}{\partial \pi}}_{A} \underbrace{- g \overline{\psi} \frac{\partial M}{\partial \pi}}_{B} + S_D + S_\varphi$$

$$= \underbrace{+g \frac{\partial [M (\psi_u - \overline{\psi})]}{\partial \pi}}_{C} \underbrace{- \left(-g M \frac{\partial \overline{\psi}}{\partial \pi} \right)}_{D} + S_D + S_\varphi$$

Malardel and Bechtold, QJRMS 2019

Mesoscale convective systems, their propagation and the diurnal cycle

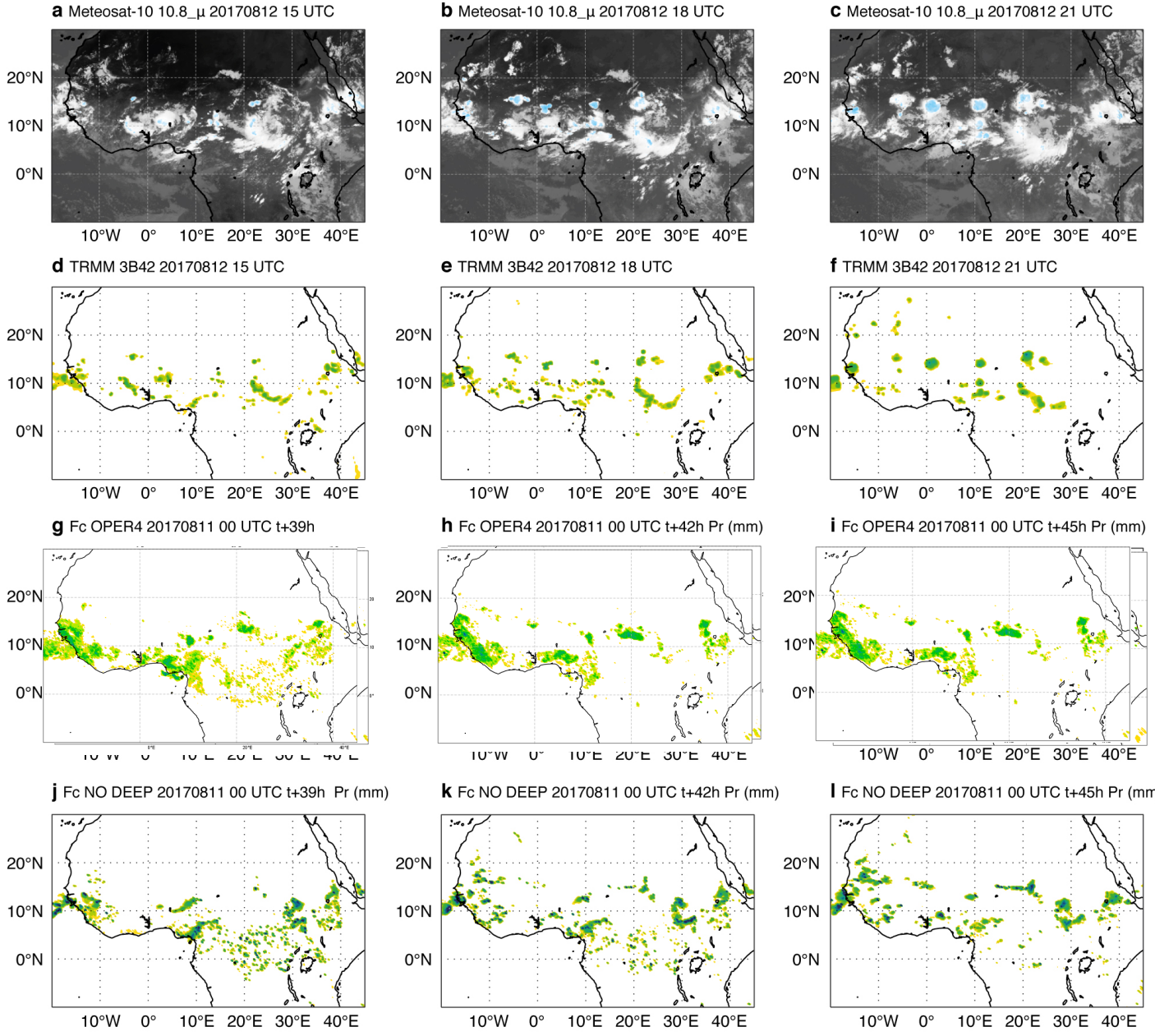

Figure: Sequence of Meteosat 10 infrared and TRMM rainfall radar sequences over Sahel and reforecast for **8 Aug 2017** at 4 km with and without deep convection parametrization

CAPE and CIN before and after precipitation

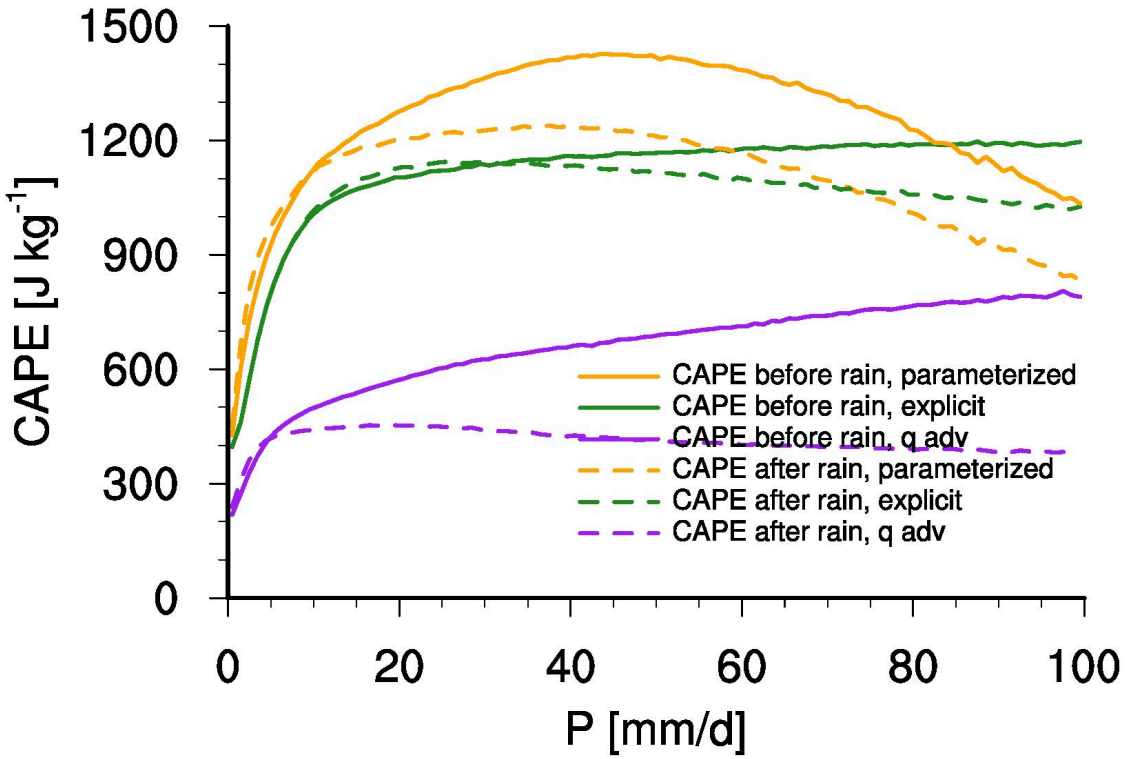

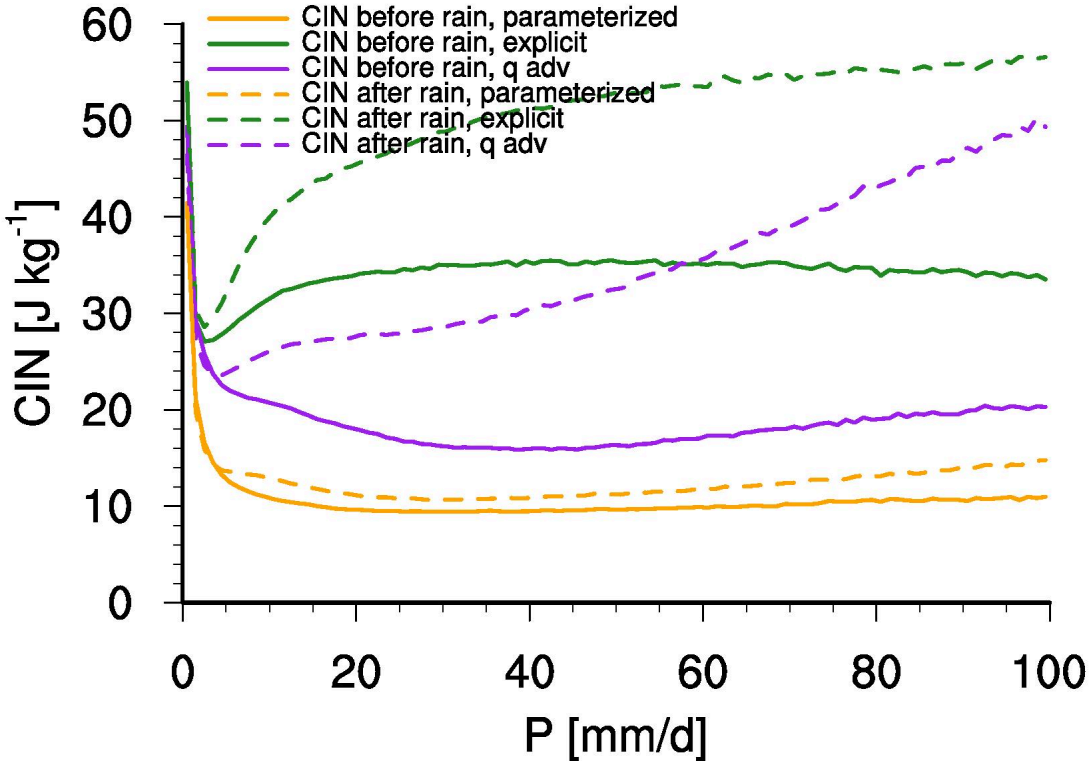

Tobias Becker

Precipitation and propagation

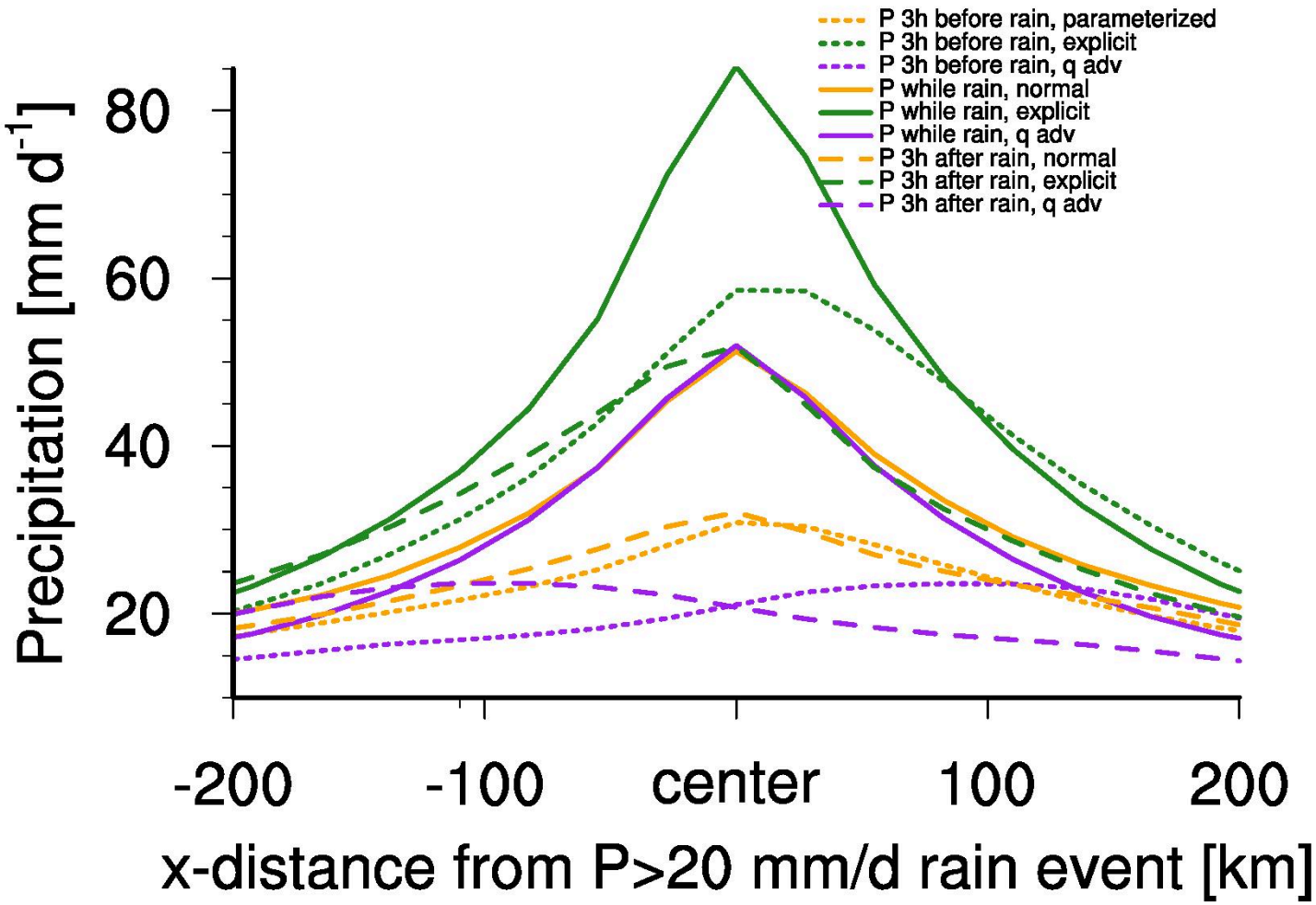

Global spectra of KE at 200 hPa for different resolutions and Precip distribution

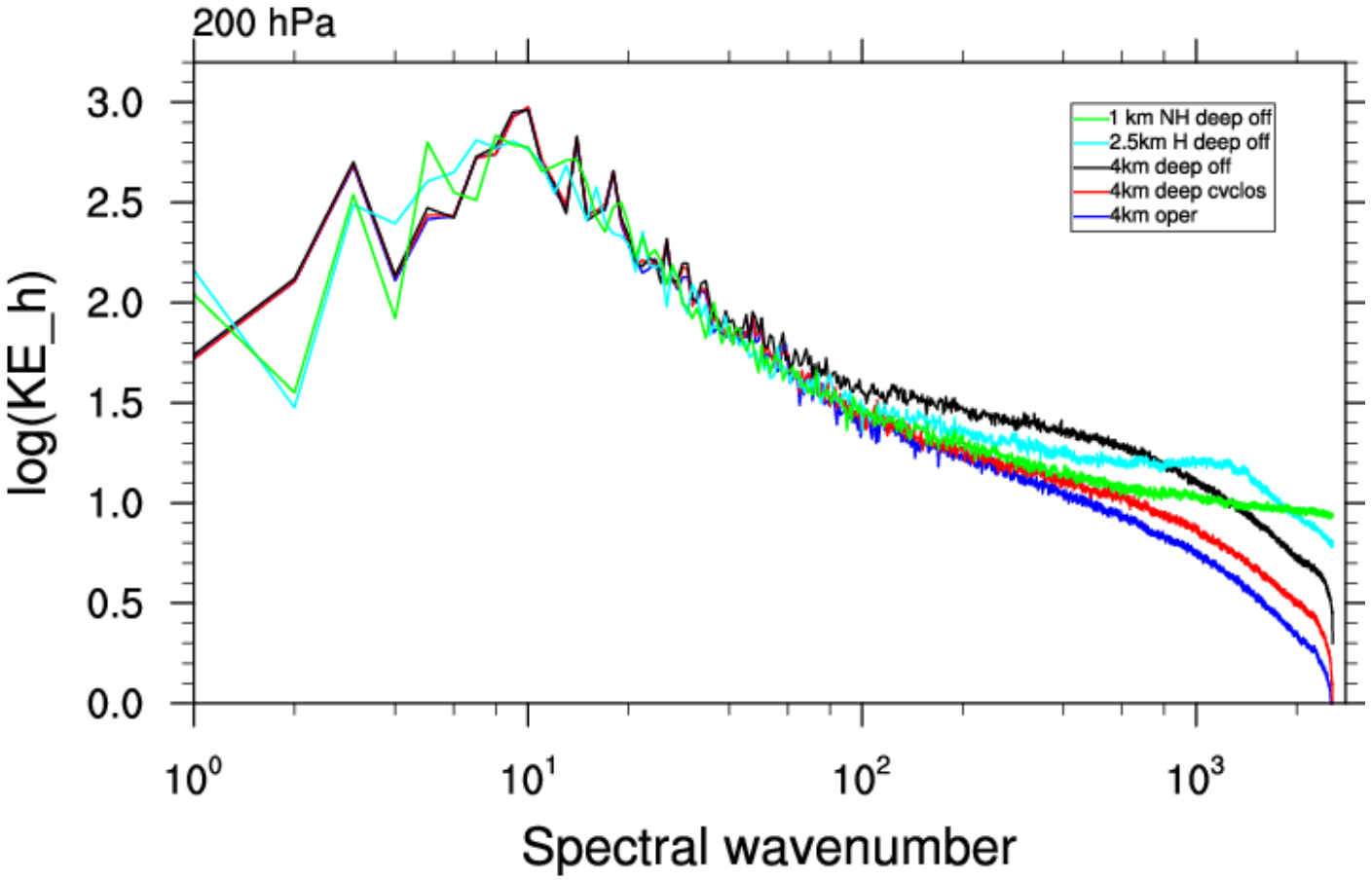

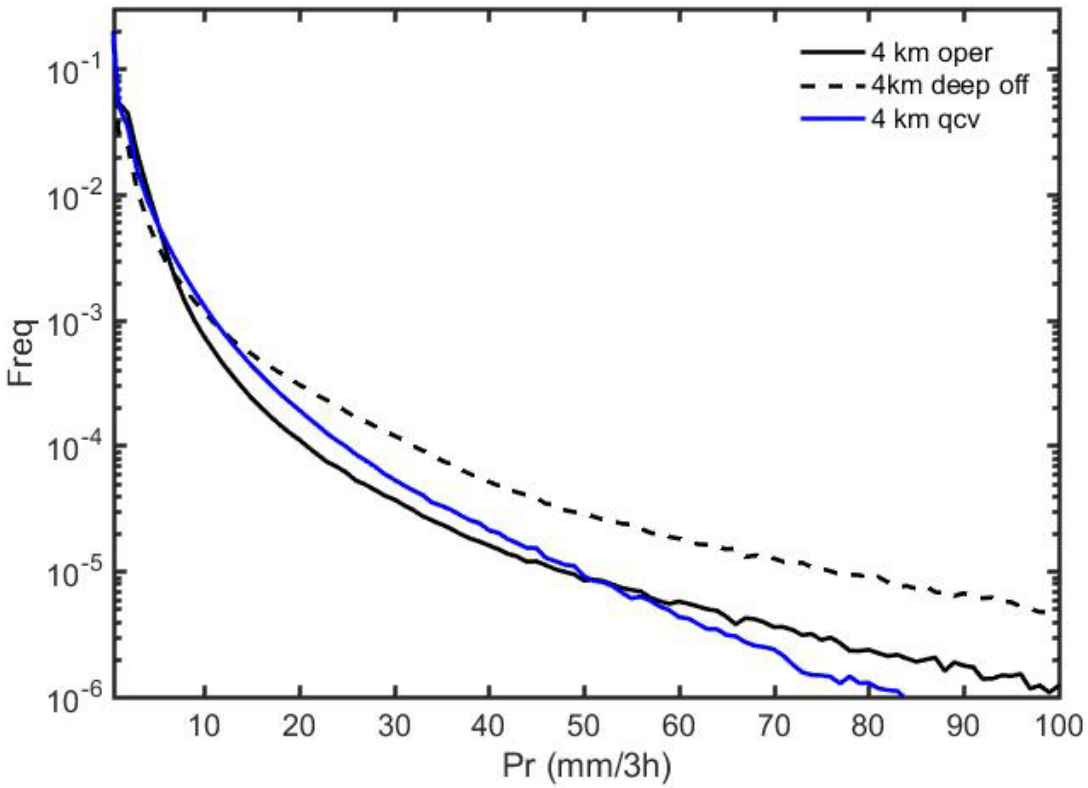

Figure . It is possible to increase KE by adapting convection parametrization (closure, coupling with dynamics), still conservative and experimental scaling, but promising especially against 1 km results.

Precipitation verification against Synop observations: **4, 9** km **deep oper vs** 4 km explicit August

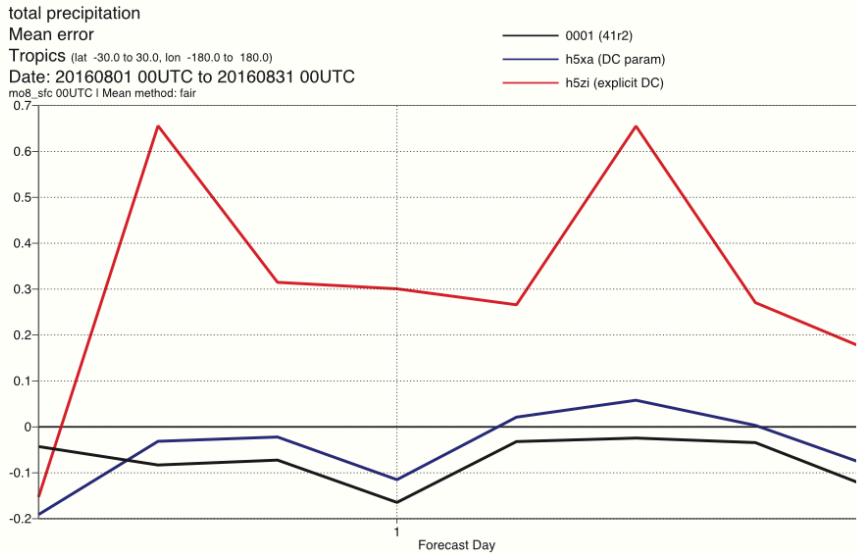

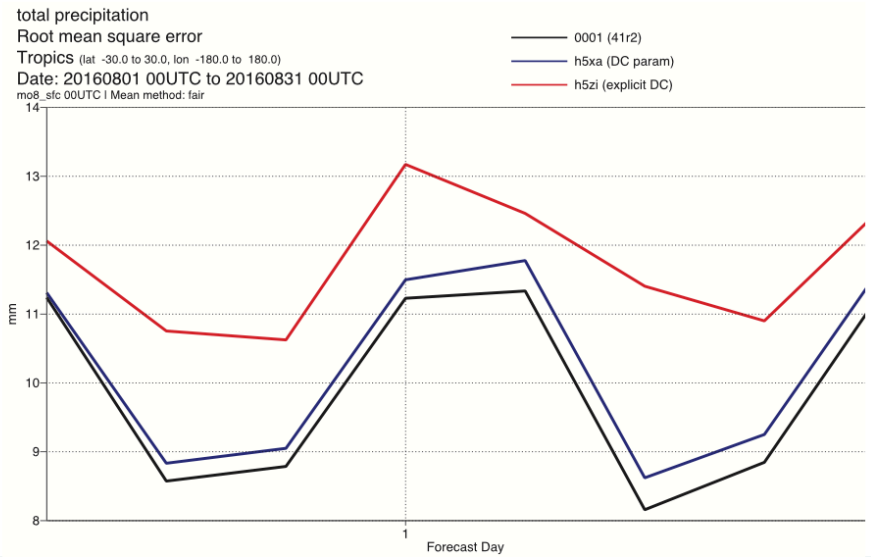

thanks to
Thomas Haiden

TCo399=32 km ensemble precipitation verification against radar: **Oper** and new conv June 2018

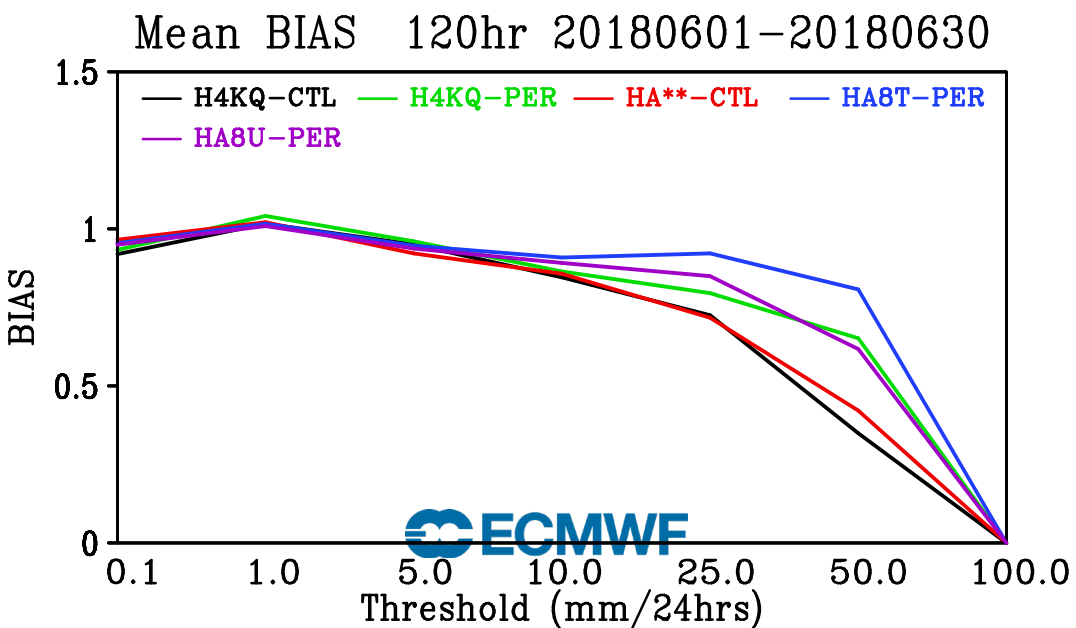

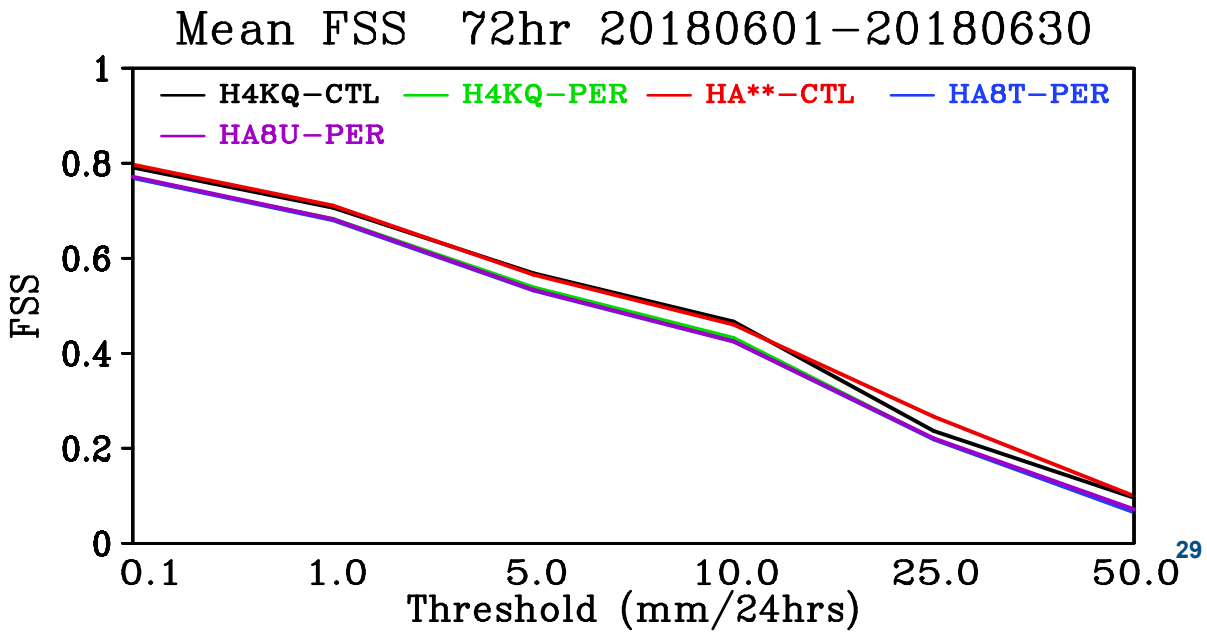

Signature of gravity waves in satellite infrared channels and model (mis)-fit

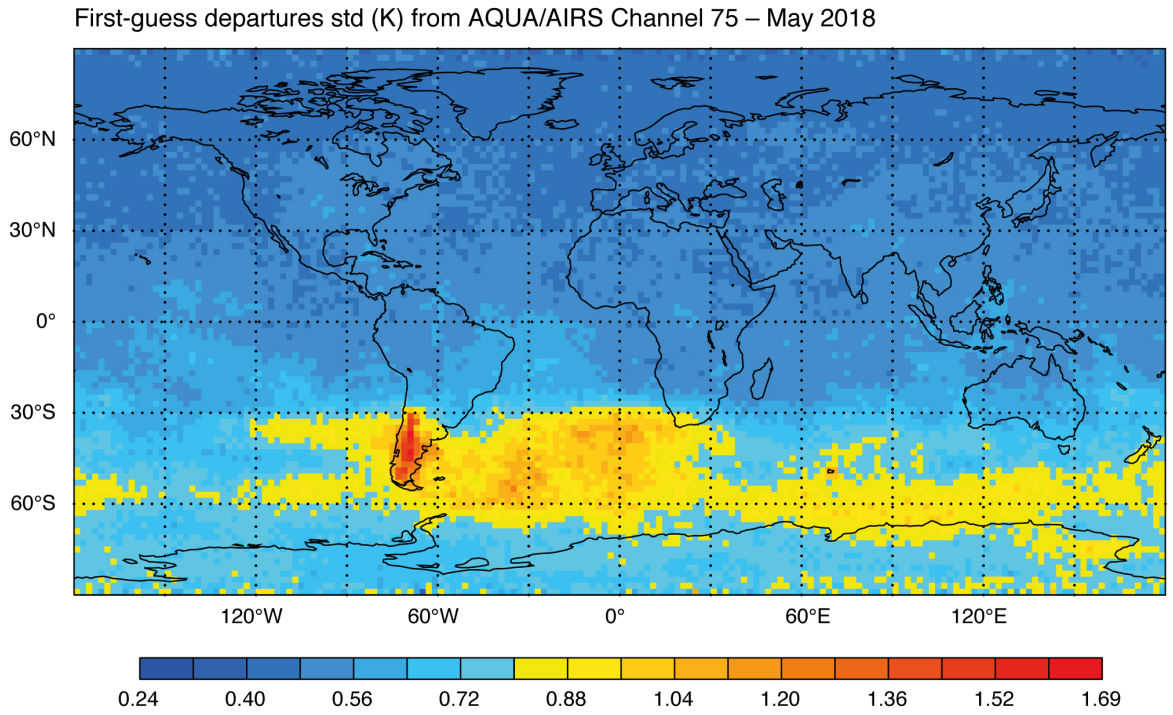

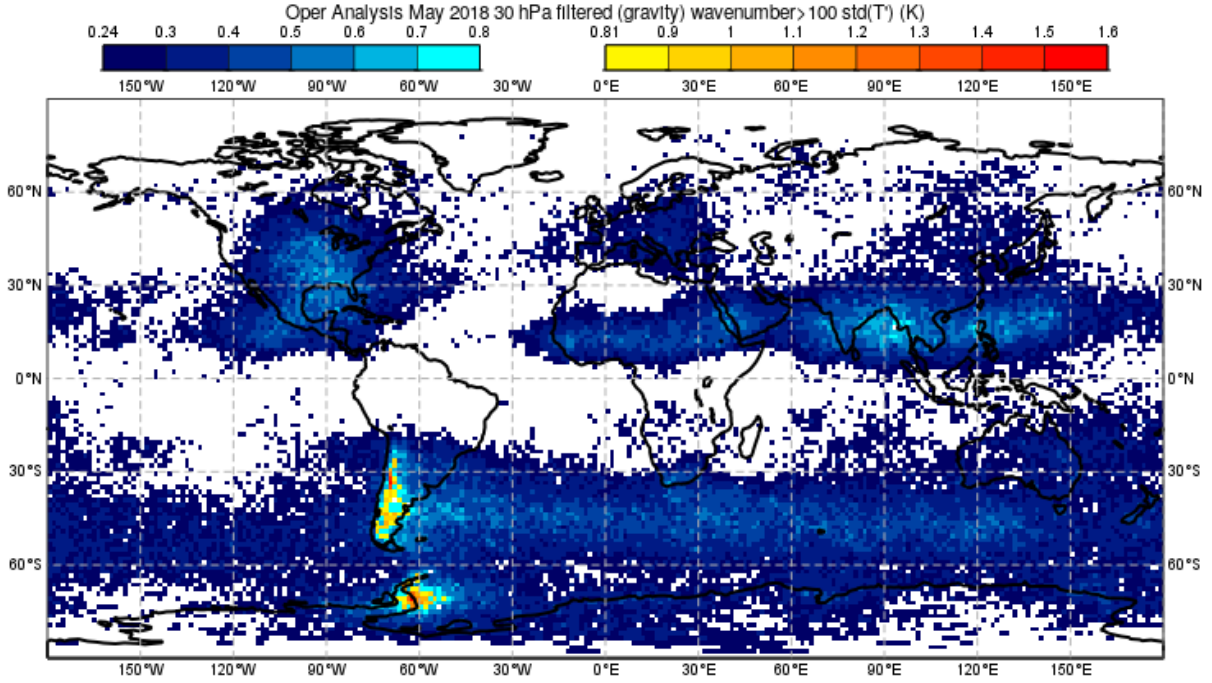

Figure. Standard deviation of first-guess temperature departures in the upper stratosphere of the IFS against the Atmospheric Infrared Sounder (AIRS) channel 75 onboard NASA's AQUA satellite during May 2018 and total wavenumber>100 filtered std(T') form the operational analysis

Stratospheric gravity wave signature: difference in analyses with more realistic convection and the tangent-linear model approximation

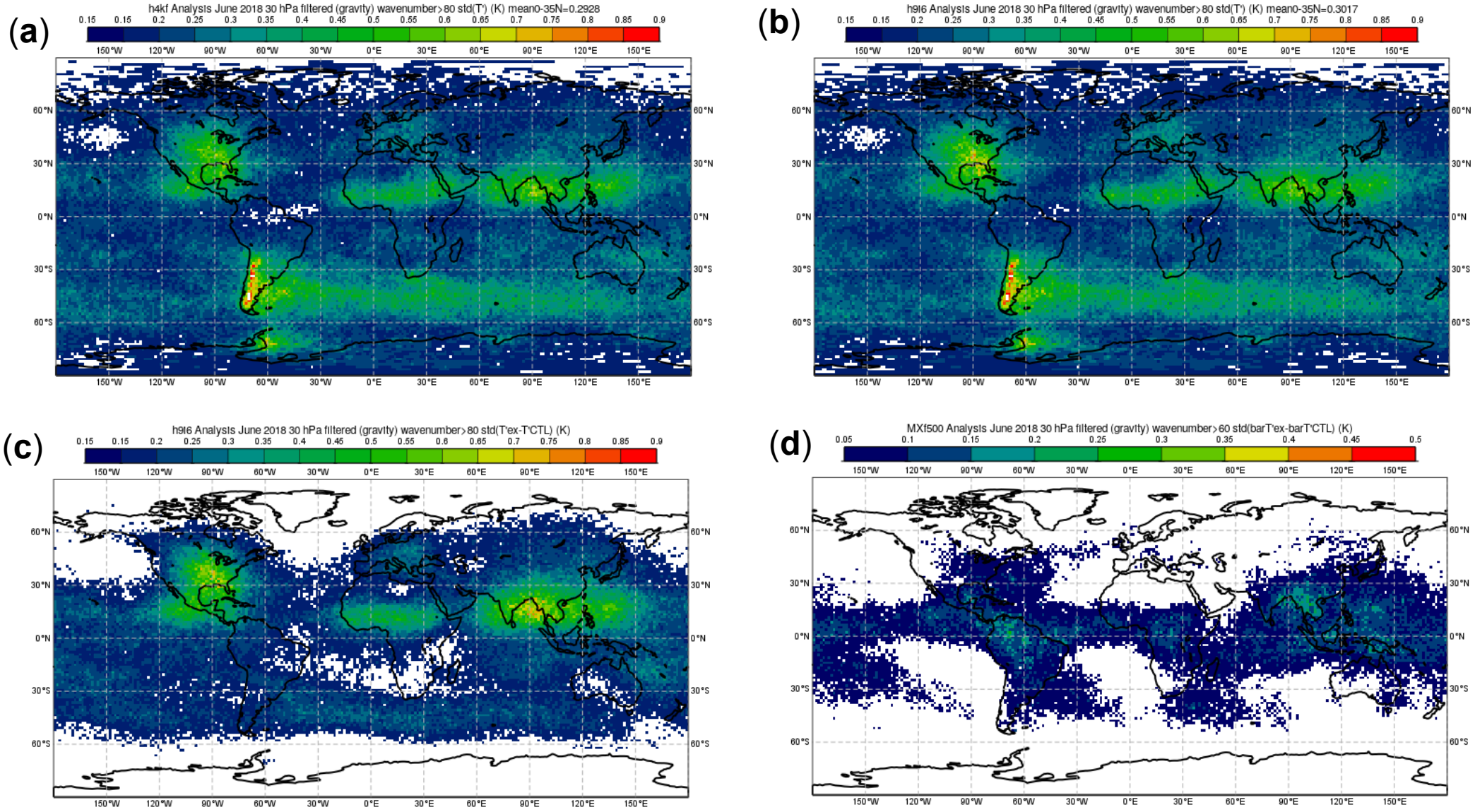

Figure. Standard deviation of wavenumber>80 filtered T' at 30 hPa for two analyses with different convection (a), (b) std of differences (c) and difference in TL and nonlinear model (d)

(Orographic) gravity waves in radiosondes and model

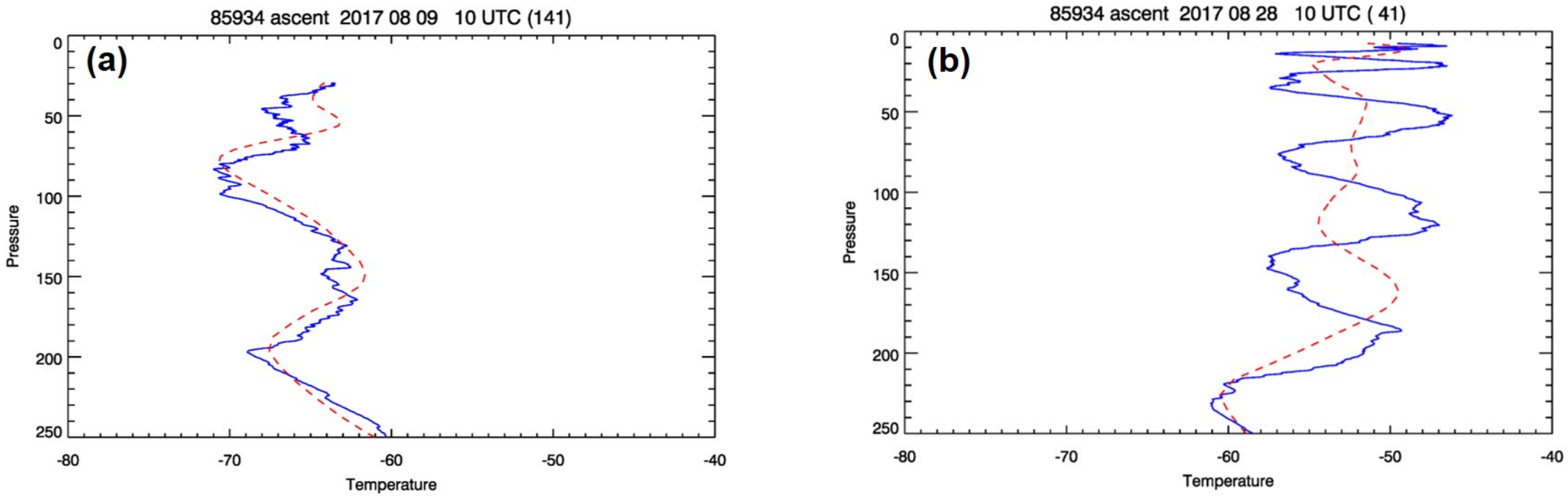

Figure. High-resolution temperature profiles above 250 hPa from radiosonde ascents at Punta Arenas in Chile (53°S, 70.84°W) for the 9 and 28 August 2017 (solid lines) and corresponding temperature profiles from the IFS short-range forecasts (dashed lines). Figure courtesy Bruce Ingleby.

Global spectra of Rot & Div at 50 hPa for different resolution

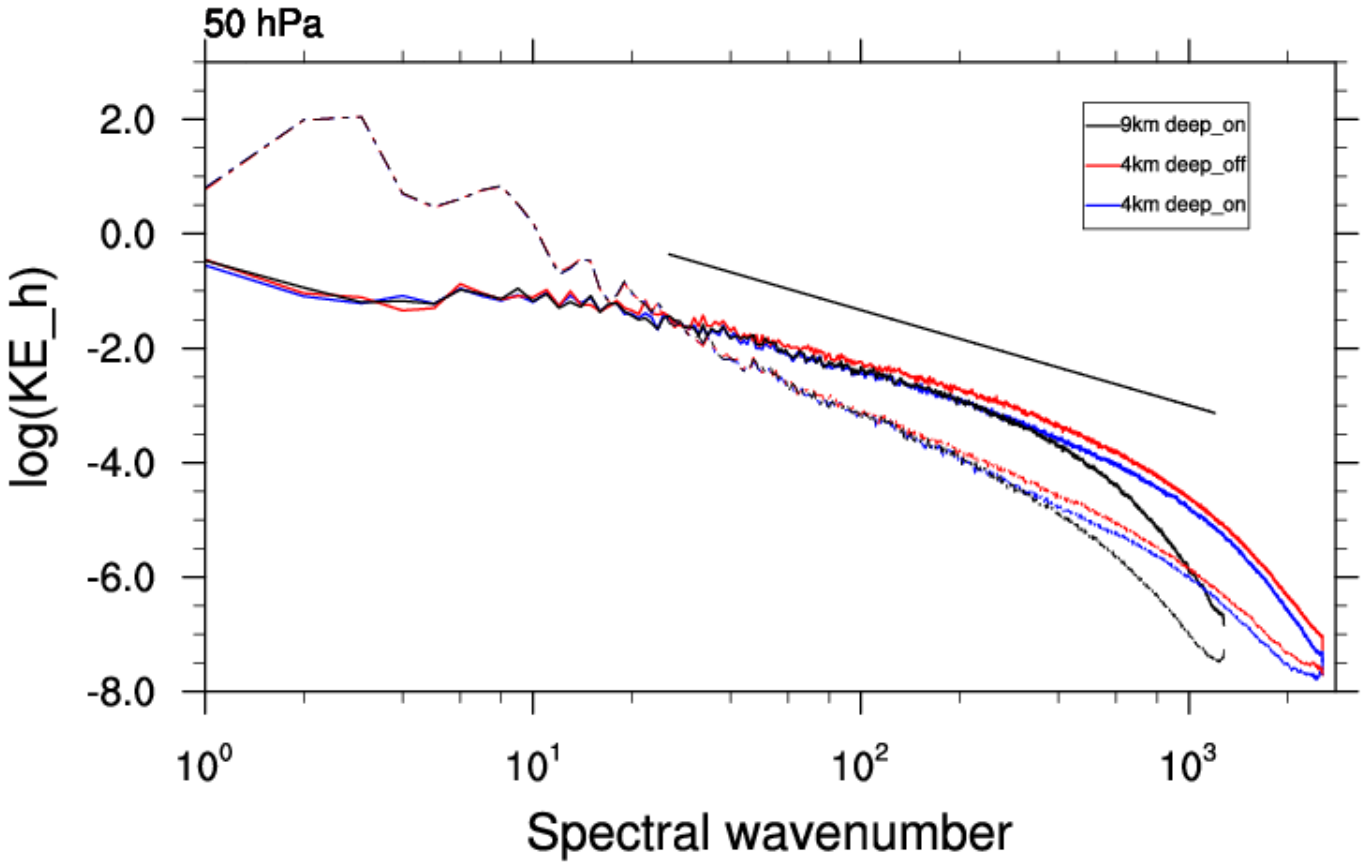

Figure. Global spectra of the rotational (dashed) and divergent part (solid) of the horizontal kinetic energy at 50 hPa as a function of the global wavenumber for different model configurations: 9 and 4 km horizontal resolutions with the deep convection scheme and 4 km without the deep convection scheme. The straight black line denotes the -5/3 spectral slope.

New products and supporting Field campaigns

CAT and MWT turbulence index derived form projection of 3D indices on eddy dissipation rate (Sharman and Pearson (2017). Real-time forecasts for **SOUTHTRACK September 2019 ,** with DLR (A. Doernbrack, M. Bramberger NCAR) and FZ Juelich (P. Preusse), and **STRATEOLE II Balloons November 2019** (M. Bramberger, J. Alexander NCAR)

ECMWF FORECASTS: 28-08-2019 00:00

ECMWF forecasts are prepared by Andreas Dörnbrack, DLR

Model: ECMWF T1279/L137 Deterministic Forecast

Initialization time (dd-mm-yyyy): 28-08-2019 00:00 UTC

Change to: 29-08-2019 00:00 Change

Patagonia: CAT Index: 206 hPa (~FL390) at +24h

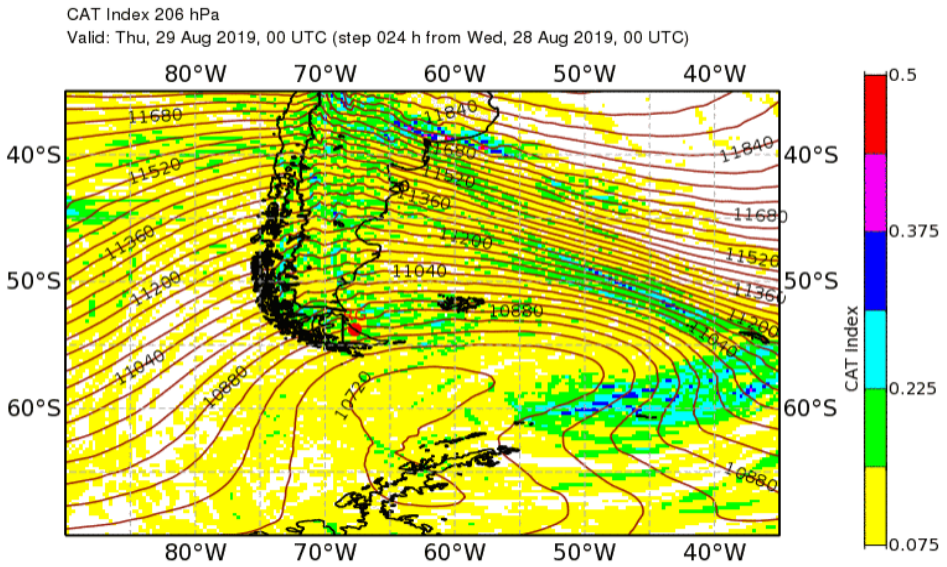

ECMWF FORECASTS: 28-08-2019 00:00

ECMWF forecasts are prepared by Andreas Dörnbrack, DLR

Model: ECMWF T1279/L137 Deterministic Forecast

Initialization time (dd-mm-yyyy): 28-08-2019 00:00 UTC

Change to: 29-08-2019 00:00 Change

Patagonia: MWT Index: 206 hPa (~FL390) at +24h

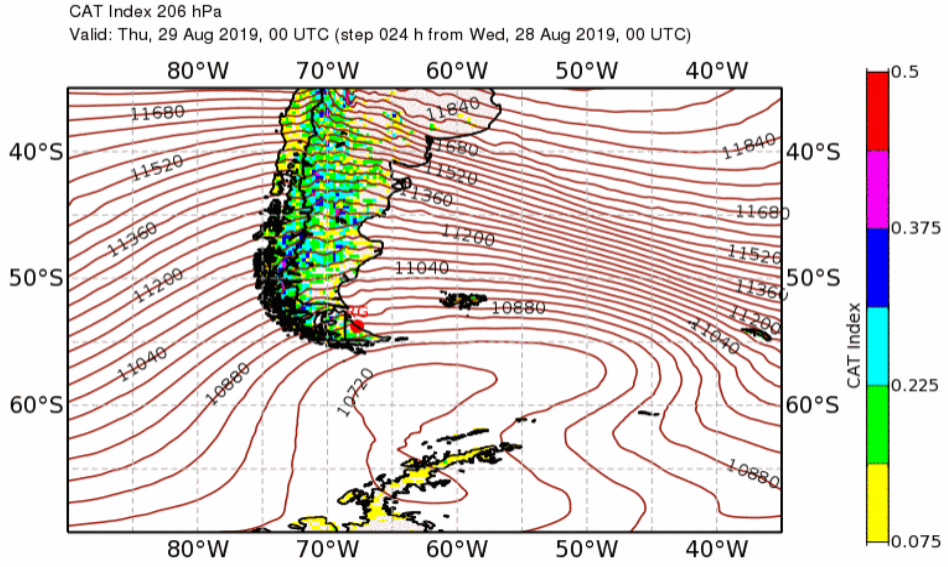

Conclusions= Challenges for model

- Getting phase and amplitude of (convective) heating right for wave modulation
- Further improve on MJO as it is one of main sources of middle latitude predictability – maritime continent barrier and coupled ocean convection/wind biases
- Diurnal cycle and night-time propagating mesoscale convective systems
- Mesoscale spectra, -5/3 but for good reasons = control the gridpoint rainfall; good spectra =/ good forecasts (correlation)
- At 4 km neither convection permitting nor parametrized is ideal, possible to get variability right with improved parametrization
- Gravity wave activity both orographic and non-orographic (convective); sources and horizontal propagation – sufficient vertical resolution needed << 1km, TL approximation, gravity wave filtering

Revision of the convective cloudy boundary-layer

- No iteration of **vertical diffusion** scheme, No statistical cloud scheme,

- Same **test parcel for convective boundary-layer height** as in convection
- Rewritten diffusion momentum solver

- Shallow convection does moist transport, improved stability of shallow convection for Stratocumulus (mass fluxes)

- Consistent coupling to cloud scheme through **detrainment and subsidence** terms

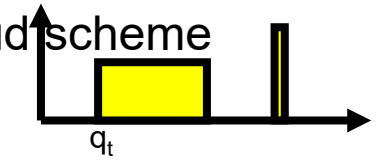

- Revised and **sequential cloud saturation adjustment** (no double call of cloud scheme)

- 6% faster IFS

frequency shallow [0-1]

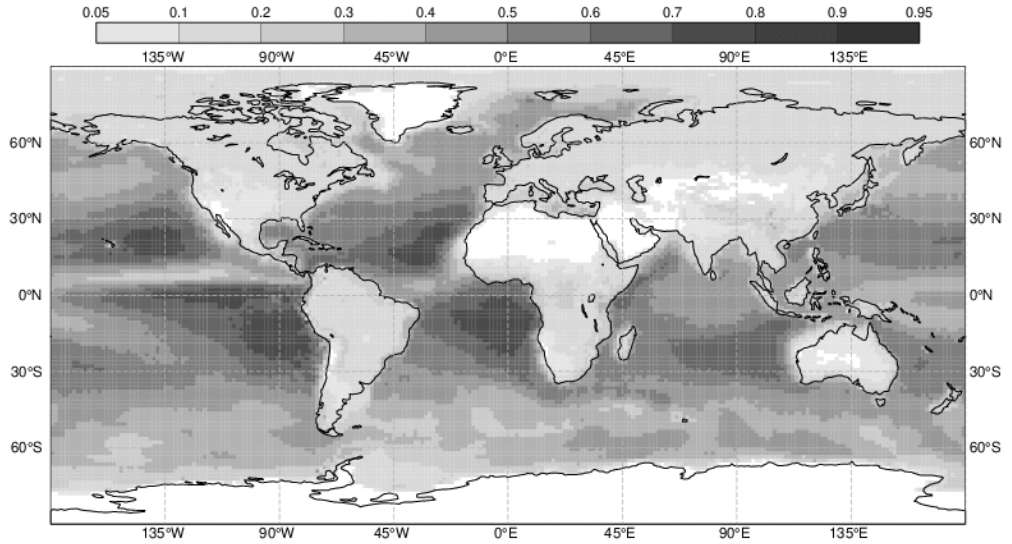

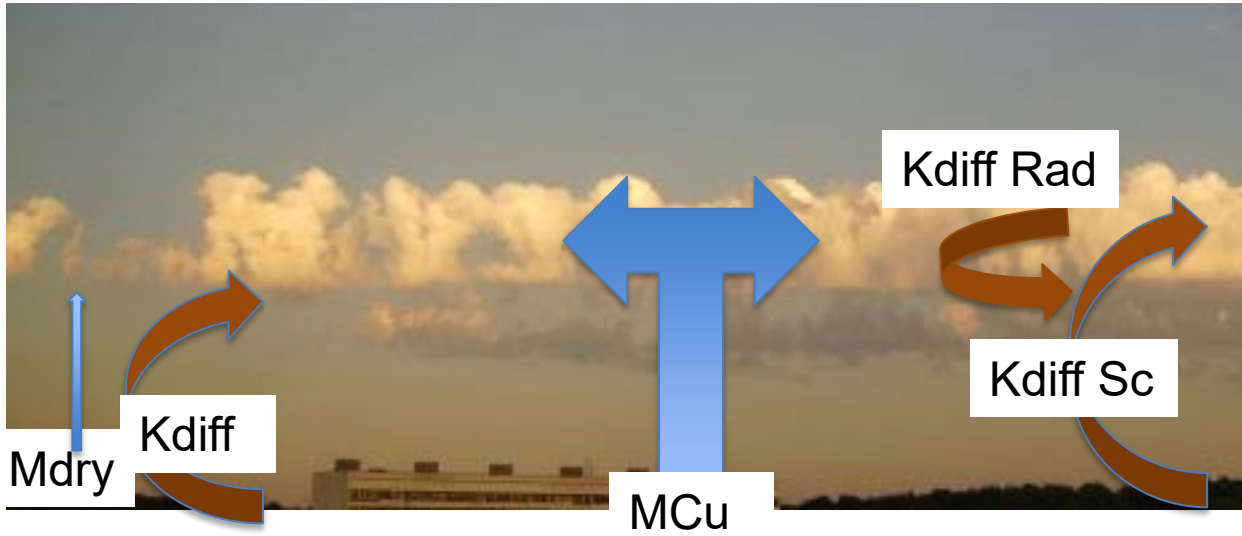

Use inversion strength –Pascal Marquet moist static energy

Direct convection-dynamics coupling: change in q-tendencies (K/day)

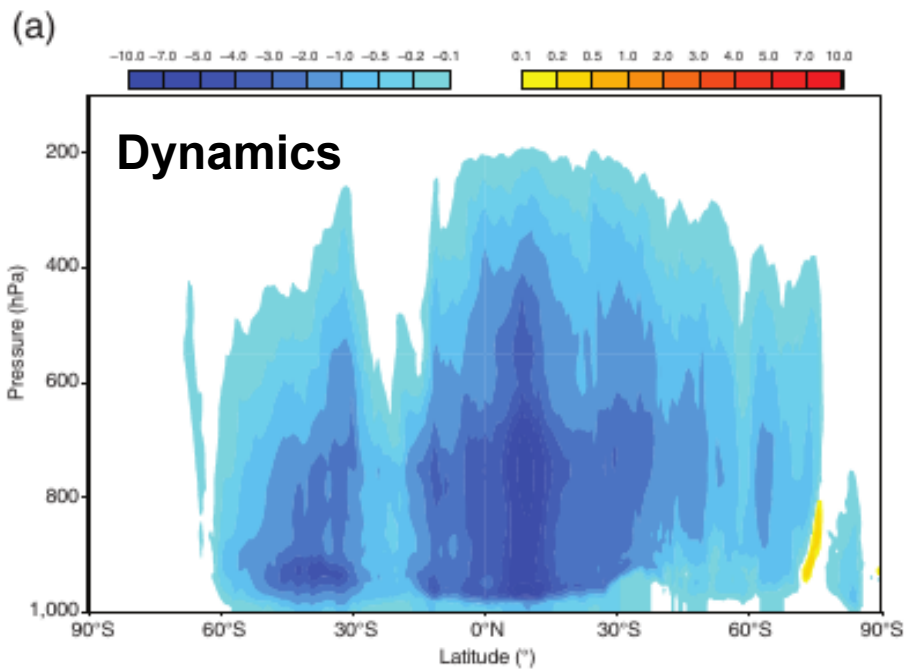

K/day

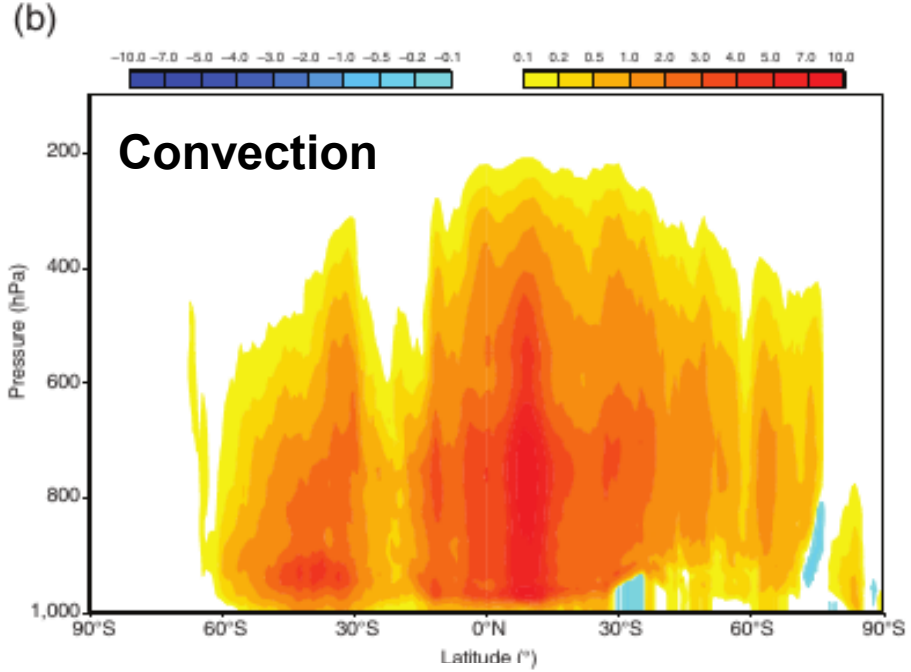

K/day

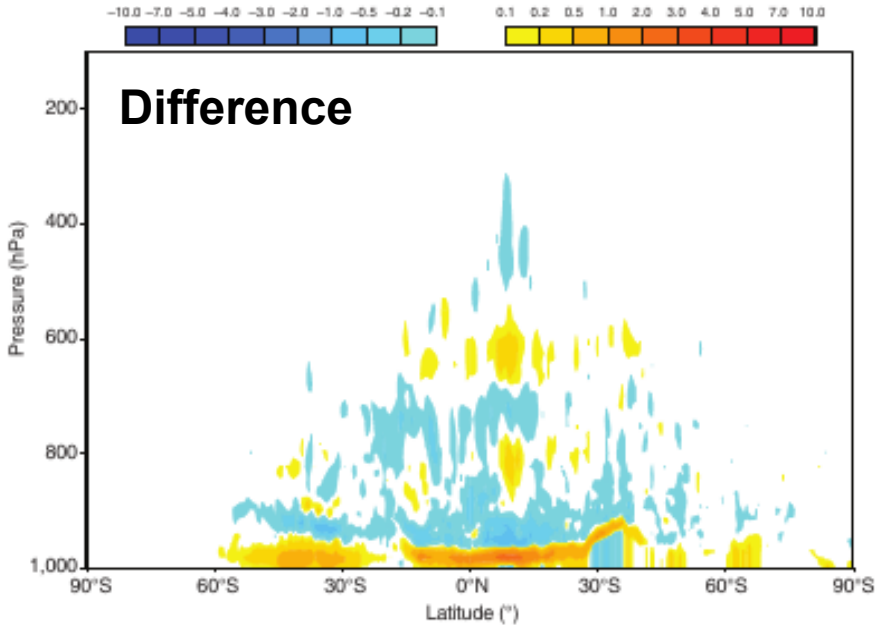

Direct convection-dynamics coupling: squall line on small Planet dx=2 km

Convection permitting

Param

Param+ coupling

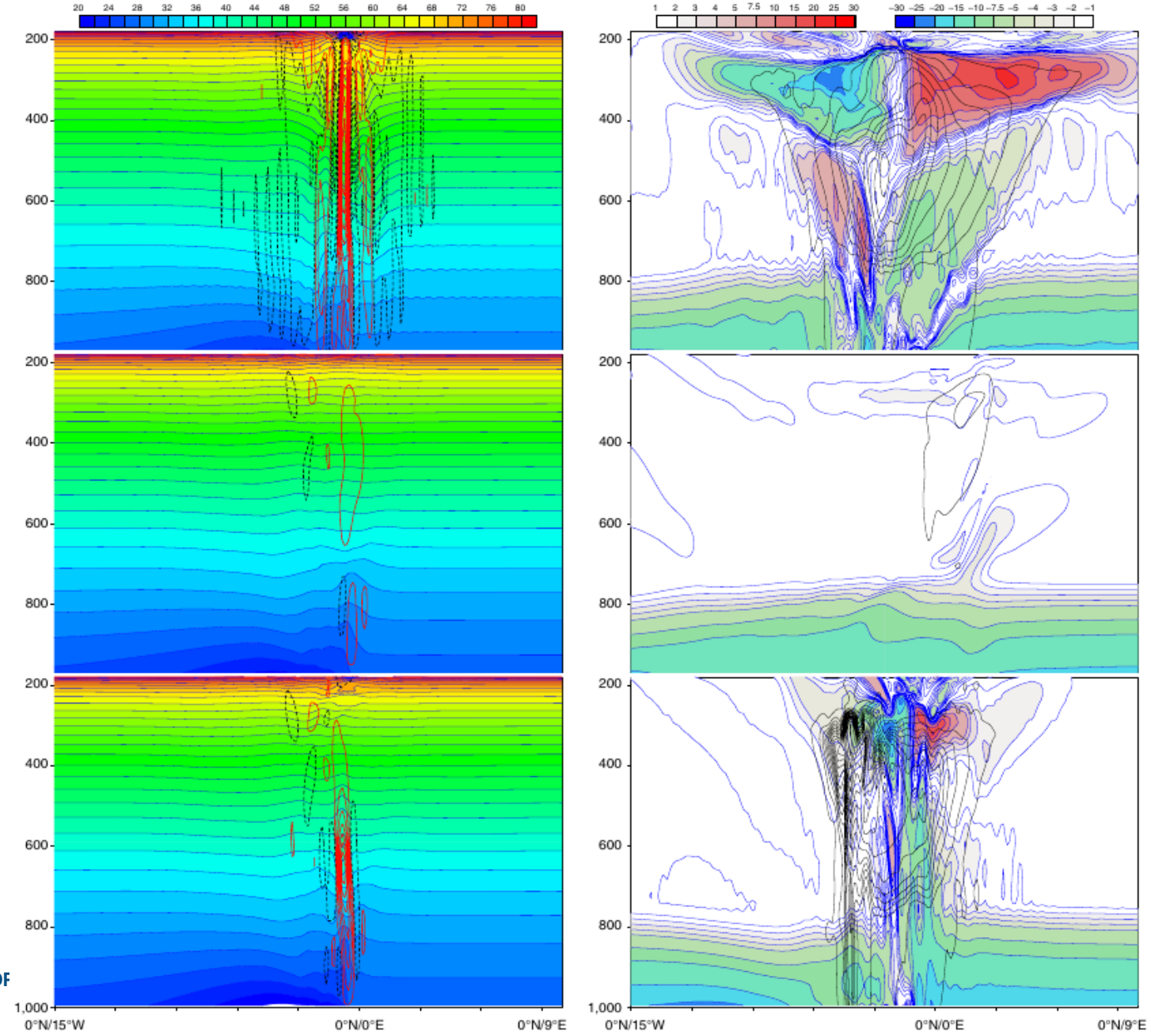

ECMWF EUROF